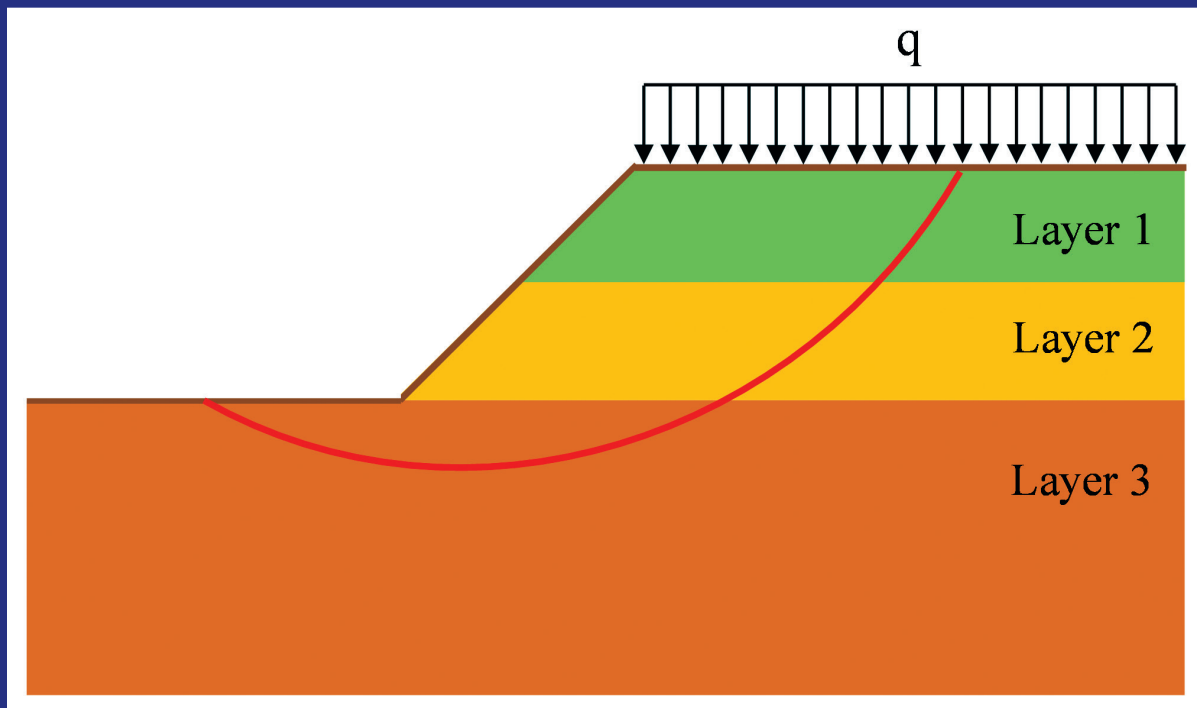


JOINT TRANSPORTATION RESEARCH PROGRAM

INDIANA DEPARTMENT OF TRANSPORTATION
AND PURDUE UNIVERSITY



Implementation of Limit States and Load Resistance Design of Slopes



Rodrigo Salgado

Faraz S. Tehrani

Sang Inn Woo

Yanbei Zhang

Monica Prezzi

RECOMMENDED CITATION

Salgado, R., S. I. Woo, F. S. Tehrani, Y. Zhang, and M. Prezzi. *Implementation of Limit States and Load Resistance Design of Slopes*. Publication FHWA/IN/JTRP-2013/23. Joint Transportation Research Program, Indiana Department of Transportation and Purdue University, West Lafayette, Indiana, 2013. doi: 10.5703/1288284315225.

AUTHORS

Rodrigo Salgado, PhD

Professor of Civil Engineering
Lyles School of Civil Engineering
Purdue University
(765) 494-5030
rodrigo@purdue.edu
Corresponding Author

Sang Inn Woo

Graduate Research Assistant
Lyles School of Civil Engineering
Purdue University

Faraz S. Tehrani

Graduate Research Assistant
Lyles School of Civil Engineering
Purdue University

Yanbei Zhang

Graduate Research Assistant
Lyles School of Civil Engineering
Purdue University

Monica Prezzi, PhD

Professor of Civil Engineering
Lyles School of Civil Engineering
Purdue University

ACKNOWLEDGMENTS

The research presented in this report was funded by the Joint Transportation Research Program at Purdue University. The authors acknowledge the financial support from the Indiana Department of Transportation and the Federal Highway Administration. Chapter 1 largely follows Salgado and Kim, 2013 (doi 10.1061/(ASCE)GT.1943-5606.0000978).

JOINT TRANSPORTATION RESEARCH PROGRAM

The Joint Transportation Research Program serves as a vehicle for INDOT collaboration with higher education institutions and industry in Indiana to facilitate innovation that results in continuous improvement in the planning, design, construction, operation, management and economic efficiency of the Indiana transportation infrastructure. https://engineering.purdue.edu/JTRP/index_html

Published reports of the Joint Transportation Research Program are available at: <http://docs.lib.purdue.edu/jtrp/>

NOTICE

The contents of this report reflect the views of the authors, who are responsible for the facts and the accuracy of the data presented herein. The contents do not necessarily reflect the official views and policies of the Indiana Department of Transportation or the Federal Highway Administration. The report does not constitute a standard, specification or regulation.

TECHNICAL REPORT STANDARD TITLE PAGE

1. Report No. FHWA/IN/JTRP-2013/23	2. Government Accession No.	3. Recipient's Catalog No.	
4. Title and Subtitle Implementation of Limit States and Load Resistance Design of Slopes		5. Report Date November 2013	
7. Author(s) Rodrigo Salgado, Sang Inn Woo, Faraz S. Tehrani, Yanbei Zhang, Monica Prezzi		6. Performing Organization Code	
9. Performing Organization Name and Address Joint Transportation Research Program Purdue University 550 Stadium Mall Drive West Lafayette, IN 47907-2051		8. Performing Organization Report No. FHWA/IN/JTRP-2013/23	
12. Sponsoring Agency Name and Address Indiana Department of Transportation State Office Building 100 North Senate Avenue Indianapolis, IN 46204		10. Work Unit No.	
15. Supplementary Notes Prepared in cooperation with the Indiana Department of Transportation and Federal Highway Administration.		11. Contract or Grant No. SPR-3375	
16. Abstract <p>A logical framework is developed for load and resistance factor design (LRFD) of slopes based on reliability analysis. LRFD of slopes with resistance factors developed in this manner ensures that a target probability of slope failure is not exceeded. Three different target probabilities of failure (0.0001, 0.001 and 0.01) are considered in this report. The ultimate limit state for slope stability (formation of a slip surface and considerable movement along this slip surface) is defined using the Bishop simplified method with a factor of safety equal to unity. Gaussian random field theory is used to generate random realizations of a slope with values of strength and unit weight at any given point of the slope that differ from their mean by a random amount. A slope stability analysis is then performed for each slope realization to find the most critical slip surface and the corresponding driving and resisting moments. The probability of slope failure is calculated by counting the number of slope realizations for which the factor of safety did not exceed 1 and dividing that number by the total number of realizations. The mean of the soil parameters is adjusted and this process repeated until the calculated probability of failure reaches to the target probability of failure. Optimal resistance and load factors are obtained by dividing the resisting and driving moments corresponding to the most probable ultimate limit state by the nominal values of resisting and driving moments.</p> <p>The main goal of this study was to provide specific values of resistance and load factors to implement in limit states and load resistance design of slopes in the context of transportation infrastructure. This report discusses the concepts of load and resistance factors, target probability of failure and the ultimate limit state equation in the context of slope stability analysis. It then presents a detailed algorithm for resistance factor calculation by using reliability analysis. Six cases of real slopes designed and constructed by INDOT are examined by using undrained shear strengths in order to illustrate the LRFD procedure and validate the recommended resistance and load factors.</p>		13. Type of Report and Period Covered Final Report	
17. Key Words slopes; slope stability; slope stability analysis; load and resistance factor design; LRFD		14. Sponsoring Agency Code	
19. Security Classif. (of this report) Unclassified		18. Distribution Statement No restriction. This document is available to the public through the National Technical Information Service Springfield, VA 22161.	
20. Security Classif. (of this page) Unclassified		21. No. of Pages 23	22. Price N/A

EXECUTIVE SUMMARY

IMPLEMENTATION OF LIMIT STATES AND LOAD RESISTANCE DESIGN OF SLOPES

Introduction

A logical framework is developed for load and resistance factor design (LRFD) of slopes based on reliability analysis. LRFD of slopes with resistance factors developed in this manner ensures that a target probability of slope failure is not exceeded. Three different target probabilities of failure (0.0001, 0.001, and 0.01) are considered in this report. The ultimate limit state for slope stability (formation of a slip surface and considerable movement along this slip surface) is defined using the Bishop simplified method with a factor of safety equal to unity. Gaussian random field theory is used to generate random realizations of the slope with values of strength and unit weight at any given point of the slope that differ from their mean by a random amount. A slope stability analysis is then performed for each slope realization to find the most critical slip surface and the corresponding driving and resisting moments. The probability of slope failure is calculated by counting the number of slope realizations for which the factor of safety did not exceed 1 and dividing that number by the total number of realizations. The mean of the soil parameters is adjusted and this process repeated until the calculated probability of failure is equal to the target probability of failure. Optimal resistance and load factors are obtained by dividing the resisting and driving moments corresponding to the most probable ultimate limit state by the nominal values of resisting and driving moments. The main goal of this study was to provide specific values of resistance and load factors to implement in limit states and load resistance design of slopes in the context of transportation infrastructure. This report introduces the concept of load and resistance factors, the target probability of failure for slopes, and the ultimate limit state equation. It then presents a detailed algorithm for resistance factor calculation by using reliability

analysis. Six slope stability cases provided by INDOT are examined in order to illustrate the LRFD procedure and validate the recommended resistance and load factors.

Findings

The main goal of this study was to provide more specific guidance on values of resistance factors to implement in load and resistance factor design of slopes, with specific illustrations.

The effect of slope geometry was investigated. It was shown that, when realistic values of COV and scale of fluctuation of the soil properties were assumed (values close to those of set D), the resulting resistance factor values did not depend strongly on slope geometry, suggesting that the rigorous reliability analysis algorithm proposed in the present study can be used effectively to produce load and resistance factors for use in design of slopes.

The LRFD methodology was used to check the stability of a total of six slope cases (cases A through F) provided by INDOT. The short-term (undrained) properties of soil were used to analyze all cases. For all the adopted target probabilities of failure, there were strong linear correlations between the ratio RF of factored resistance to factored load and FS .

Based on this study, the recommended resistance factors RF^* adjusted with respect to the proposed load factors LF^* ($LF_{DL}^* = 1.0$ and $LF_{LL}^* = 1.2$) are 0.75, 0.70, and 0.65 for $P_{f,T}$ of 0.01 (1%), 0.001 (0.1%), and 0.0001 (0.01%), for undrained slopes respectively.

Implementation

INDOT should start using the load and resistance factors proposed in this research project in slope stability checks in INDOT projects. As confidence in the application develops, greater reliance on this very economical method of checking slope stability will follow. Research opportunities for improvement of these factors should be pursued.

CONTENTS

1. INTRODUCTION	1
1.1. Load and Resistance Factors	1
1.2. Target Probability of Failure for Slopes	2
1.3. Ultimate Limit State Equation	2
1.4. Algorithm for Resistance Factor Calculation using Reliability Analysis	3
1.5. Calculation Example	4
1.6. Case Studies	5
1.7. Application to Design Code Development	6
1.8. Degree of Conservatism of Results	7
1.9. Impact of Geometry	8
2. FURTHER VALIDATION IMPLEMENTATION OF RESISTANCE AND LOAD FACTORS	9
2.1. Implementation	9
2.2. Results	9
3. SUMMARY AND CONCLUSIONS	18
REFERENCES	18

LIST OF TABLES

Table	Page
Table 1.1 Acceptable probability of failure of slopes	3
Table 1.2 Nominal values of c (s_u), ϕ , γ and the corresponding resistance and load factors, equivalent factor of safety, and the adjusted resistance factors for load factors $LF^*_{DL} = 1.0$ and $LF^*_{LL} = 1.55$ for three target probabilities of failure and the slope of Figure 1.5 subject to a surcharge of zero or 12 kN/m/m.	6
Table 1.3 Resistance factors and equivalent factor of safety values for different combinations (sets A to D) of COV values and scales of fluctuation of c (s_u), ϕ , and γ corresponding to load factors $LF^*_{DL} = 1.0$ and $LF^*_{LL} = 1.2$	8
Table 1.4 Comparison between resistance factors and equivalent factor of safety values for combination sets D ($COV_{c(su)} = 0.2$; $COV_\gamma = 0.05$; $s_f = 10\text{m}$) for the proposed $LF^*_{DL} = 1.0$ and $LF^*_{LL} = 1.2$ for different slope geometries and soil layer conditions (for undrained slope analyses)	8
Table 2.1 Range and selected values of adjusted resistance factors RF^* for the proposed load factors ($LF^*_{DL} = 1.0$ and $LF^*_{LL} = 1.2$) with respect to the failure probability $P_{f,T}$	9
Table 2.2 Soil profile for each case	16
Table 2.3 Geometry of the six slopes	16
Table 2.4 Factors of safety from STABL [®] and Geoslope 2007 [®] for each case	16
Table 2.5 Analysis results for $P_{f,T} = 0.01$	17
Table 2.6 Analysis results for $P_{f,T} = 0.001$	17
Table 2.7 Analysis results for $P_{f,T} = 0.0001$	18

LIST OF FIGURES

Figure	Page
Figure 1.1 Failure surface, failure point, and equiprobable ellipses of two random variables	1
Figure 1.2 Geometry of a three-layer soil slope	4
Figure 1.3 Scatter of driving moments $M_{d,DL}/r_{slip}$ and $M_{d,LL}/r_{slip}$ and resisting moment M_r/r_{slip} and the ULS surface (the grey plane is the ULS surface and the points below the ULS surface correspond to points with loading exceeding resistance)	5
Figure 1.4 Distribution of FS value for the calculation example	5
Figure 1.5 Geometry of a three-layer soil slope and initial values of its soil properties	6
Figure 1.6 Geometry of a two-layer soil slope with different slope angles (used for undrained slope cases only)	8
Figure 2.1 Cross-section view of the slope in case A	10
Figure 2.2 Cross-section view of the slope in case B	11
Figure 2.3 Cross-section view of the slope in case C	12
Figure 2.4 Cross-section view of the slope in case D	13
Figure 2.5 Cross-section view of the slope in case E	14
Figure 2.6 Cross-section view of the slope in case F	15
Figure 2.7 Schematic diagram of target slopes	16
Figure 2.8 Ratio R_f versus FS for $P_{f,T} = 0.01$ (1%)	16
Figure 2.9 Ratio R_f versus FS for $P_{f,T} = 0.001$ (0.1%)	17
Figure 2.10 Ratio R_f versus FS for $P_{f,T} = 0.0001$ (0.01%)	18

1. INTRODUCTION

1.1 Load and Resistance Factors

The main goal of slope design is to select the most economical and safest geometry, which includes angle and height of the slope. Traditionally, working stress design has been used for evaluating the stability of slopes, with a minimum factor of safety FS_{req} that must be matched or exceeded. The main shortcoming of this approach is that the values of FS_{req} are fairly consistent, even for different types of slope, regardless of (1) the geometry of the slope and (2) the degree of uncertainty associated with loads inducing instability of the slope and the resistance against the loads. As an illustration, the minimum FS values recommended in the AASHTO bridge design specifications (2) are 1.3 for soil and rock parameters, 1.8 for abutments supported above a retaining wall, and 1.5 otherwise.

Recently, load and resistance factor design has gained attention in geotechnical engineering due to the possibility that it offers of a more rational and economical design of foundations (e.g., Basu and Salgado (16)) and geotechnical structures. However, this possibility depends upon the degree of rigor in the development of LRFD methods. Development of LRFD for slopes is computationally expensive, but once a well-established LRFD method for slopes is available, it will provide a more consistent and reliable means of achieving safety in slope design than working stress design.

LRFD is based on preventing events in which the sum of factored loads exceeds the factored resistance:

$$(RF)R_n \geq \sum (LF_i)Q_{i,n} \quad (1.1)$$

where RF and LF_i are the resistance and load factors, R_n is the nominal resistance, and $Q_{i,n}$ is the nominal (or design) load.

In methods such as the Bishop Simplified Method, loading in slope stability calculations is expressed through driving moments. The driving moment due to dead loads, denoted by $M_{d,DL}$, originates from self-weight of a potential sliding mass or permanent external loads acting on the boundary of the sliding mass. The driving moment due to live loads, denoted by $M_{d,LL}$, originates from nonpermanent loads on the crest of the slope, such as vehicular loads. Resistances are expressed through a resisting moment M_r . In terms of driving and resisting moments, inequality (1.1) becomes:

$$(RF)M_{rn} \geq \sum (LF_i)M_{di,n} \quad (1.2)$$

where the summation term would generally contain terms due to permanent (dead) loads, live loads and other load sources, such as seismic forces. In this report, it contains only two terms, one due to dead and the other to live loads.

The nominal resisting and driving moments are calculated in a deterministic analysis using a limit equilibrium method, such as the Bishop simplified method, which has been shown, using limit analysis, to

produce accurate results under the most varied conditions (3–6). An ultimate limit state (ULS) surface (i.e., “failure” surface) of a slope is a surface for which M_r is equal to the sum of $M_{d,DL}$ and $M_{d,LL}$. Therefore, each point on the failure surface is a triple of variables M_r , $M_{d,DL}$, and $M_{d,LL}$ leading to $FS = 1$.

Considering now a slope with expected $FS > 1$ (so with expected values of the three moment variables within the failure surface), if the moments were deterministic variables, then the chance of the slope attaining failure (i.e., reaching $FS \leq 1$) would be zero. If the variables are instead random variables, there is a nonzero probability of $FS \leq 1$, as unfavorable deviations of the variables from their means will place the triple on or outside the failure surface. This is illustrated graphically by Figure 1.1 for the very simple case of only two variables (resistance R and load Q). Each of the ellipses shown in the figure is a locus of pairs of the two variables corresponding to the same level of deviation from their expected values. If that deviation is large enough, the ellipse becomes tangential to the failure surface at one point, represented by the point FP (for failure point, also known as design point) in Figure 1.1. If the ellipse that is tangential to the failure surface corresponds to a large deviation from the point representing the means of the two variables, then the probability of failure (the probability of attainment of the limit state as defined by the failure surface) is small, and vice-versa.

Resistance and load factors are calculated with reference to the most probable ULS and the mean state and are linked to the probability of failure associated with these two states. For example, referring to Figure 1.1, the resistance and load factors for the case depicted in the figure are:

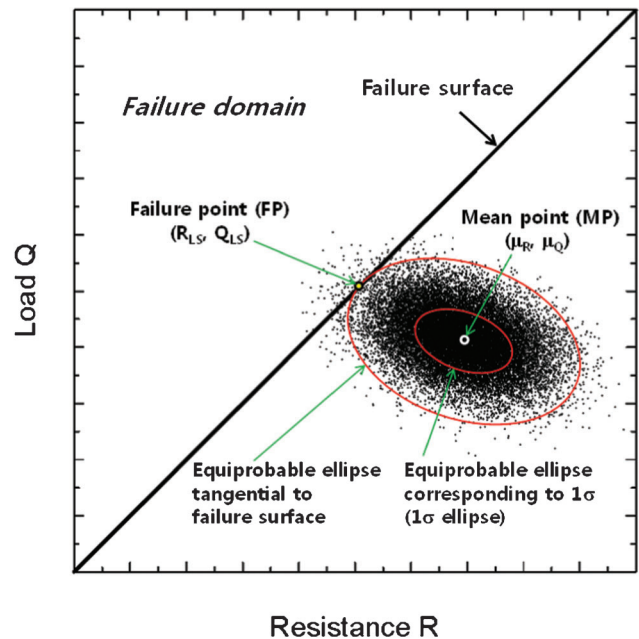


Figure 1.1 Failure surface, failure point, and equiprobable ellipses of two random variables.

$$RF = \frac{R_{LS}}{\mu_R} \quad \text{and} \quad LF = \frac{Q_{LS}}{\mu_Q} \quad (1.3)$$

where R_{LS} and Q_{LS} are the resistance and load at the most probable ULS (or failure point FP); μ_R and μ_Q are the means of resistance and load, respectively.

Using the same general procedure discussed in connection with Figure 1.1, the load and resistance factors are obtained by taking the ratios of the most probable ULS values (the values at the design point) of the resisting moment M_r , the driving moment $M_{d,DL}$ caused by dead loads and the driving moment $M_{d,LL}$ caused by live loads to their respective nominal values. Mathematically, the resistance factor RF^* and load factors LF_{DL}^* and LF_{LL}^* are given by:

$$RF^* = \frac{M_r|_{LS}}{M_r|_n}, \quad LF_{DL}^* = \frac{M_{d,DL}|_{LS}}{M_{d,DL}|_n}, \quad (1.4)$$

$$\text{and } LF_{LL}^* = \frac{M_{d,LL}|_{LS}}{M_{d,LL}|_n}$$

where $M_r|_{LS}$ is the M_r at the most probable ULS; $M_{d,DL}|_{LS}$ and $M_{d,LL}|_{LS}$ are the $M_{d,DL}$ and $M_{d,LL}$ at the most probable ULS, respectively; $M_r|_n$ is the nominal M_r ; $M_{d,DL}|_n$ and $M_{d,LL}|_n$ are the nominal $M_{d,DL}$ and $M_{d,LL}$.

The nominal values of the moments follow directly from a deterministic slope stability analysis performed with the nominal values of the problem variables (shear strength parameters and unit weight for each soil constituting the slope and any surcharge applied on the boundaries of the slope). The nominal values of these variables are their mean divided by any bias factor considered. The resistance factors calculated using Equation (1.4) correspond to the probability of failure P_f of the slope defined by the mean values of the problem variables and their probability distribution. If slope design is to be performed for a target probability of failure $P_{f,T}$ and $P_{f,T}$ is different from P_f , then the resistance factors will not be useful for an engineer attempting to use the resistance factors in design. This means that, with the goal of obtaining resistance factors that will be useful in slope design, an adjustment to the nominal values of the problem variables is required until P_f results equal to $P_{f,T}$. The next question, always from the point of view of developing values of resistance factors for use in design, is what a suitable value of $P_{f,T}$ should be.

1.2 Target Probability of Failure for Slopes

The probability of failure (P_f) of a given system, which is in reality the probability that the system either attains or goes beyond a limit state defined according to some criterion (a “failure” criterion, which can be represented in variable space as a line for two variables, a surface for three variables, or a hyper-surface for four or more variables). Adjustments to properties of the

system can make the system just so that it meets a set target probability of failure ($P_{f,T}$).

In geotechnical engineering, $P_{f,T}$ varies according to how important the structure is and how serious the consequences of attaining the limit state would be. In this context, the concept of risk may be understood in terms not only of the likelihood that certain events will occur but also of what these events consist of and what they would lead to in terms of casualties, environmental damage, financial losses, and other undesirable outcomes. Chowdhury and Flentje (7) suggested maximum values for P_f of natural slopes in a range of 0.001 to 0.15, depending on potential failure modes and the consequences of slope failure. This approach is generally similar to traditional working stress design practice, according to which different factors of safety are used depending on the importance of the structure or the quantity and quality of the data used in the design. Christian et al. (8) suggested that a typical $P_{f,T}$ for slope design purposes is 0.001 but that, for design of slopes of less importance, a greater $P_{f,T}$ (0.01) may be used. Loehr et al. (9) set the range of $P_{f,T}$ from 0.001 to 0.01 for slopes: 0.01 for relatively low potential risk and 0.001 for high potential risk. An effort was made to determine an acceptable P_f for slopes by Santamarina et al. (10) by surveying engineers involved in slope stability analysis. The results are summarized in Table 1.1.

It is still not easy for engineers to reason in terms of probability of failure and, indeed, to agree on what “failure” is. Interview with INDOT engineers revealed that there have been three “deep-seated failures,” taken to mean failures that are more serious than surface raveling or other rather shallow slope failures that are easily repaired, out of a few thousand slopes constructed in the past ten years or so. This would suggest that INDOT has been working with a failure probability of 0.001 or less, and that this appears to be acceptable.

Three different $P_{f,T}$ values (0.0001, 0.001 and 0.01) cover the range of interest in slope stability analysis in practice.

1.3 Ultimate Limit State Equation

The ULS for slopes in this study is defined based on Bishop’s simplified method (BSM) (11). Limit equilibrium methods differ in their assumption about inter-slice forces and the shape of the slip surface. BSM assumes that the vertical resultant of the inter-slice forces on the two sides of each slice is equal to zero and only considers the horizontal components in the calculation of M_r , $M_{d,DL}$, and $M_{d,LL}$. Despite the different assumptions regarding inter-slice forces, the calculated FS using BSM is comparable to those using more rigorous methods, such as Spencer’s method (12), for circular slip surfaces. Because BSM analyses are faster than Spencer analyses, given the large number of analyses required, we have used BSM in this study.

TABLE 1.1
Acceptable probability of failure of slopes (after (10))

Conditions	Acceptable P_f
Temporary structures: no potential life loss, low repair cost	0.1
Minimal consequences of failure: high cost to reduce the probability of failure (bench slope or open pit mine)	0.1–0.2
Minimal consequences of failure: repairs can be done when time permits (repair cost is less than cost of reducing probability of failure)	0.01
Existing large cut on interstate highway	0.01–0.02
Large cut on interstate highway to be constructed	<0.01
Lives may be lost when slopes fail	0.001
Acceptable for all slopes	0.0001
Unnecessarily low	<0.00001

The FS for BSM is (11,13):

$$FS_{BSM} = \sum_{i=1}^n \frac{c_i b_i + (W_i + Q_i - U_i) \tan \phi_i}{\cos \alpha_i \left(1 + \frac{\tan \alpha_i \tan \phi_i}{FS_{BSM}} \right)} \quad (1.5)$$

$$\left[\sum_{i=1}^n (W_i + Q_i) \sin \alpha_i \right]^{-1} \quad (i = 1, 2, \dots, n)$$

where n is the total number of slices, c is the cohesive intercept of the strength envelope assumed for the soil (equal to the undrained shear strength s_u when $\phi = 0$) on the base of each slice, ϕ is the friction angle along the base of the slice, b is the width of the slice, W is the weight of the slice, Q is the external load acting on top of the slice, U is the vertical water force acting on the base of the slice (equal to pore pressure times the horizontal projected area of the base of the slice), and α is the angle with the horizontal of the base of the slice.

For the development of LRFD for slopes, the ULS equation follows from setting $FS = 1$ in Equation (1.5):

$$\sum_{i=1}^n \frac{c_i b_i + (W_i + Q_i - U_i) \tan \phi_i}{\cos \alpha_i (1 + \tan \alpha_i \tan \phi_i)} - \sum_{i=1}^n (W_i + Q_i) \sin \alpha_i = 0 \quad (1.6)$$

1.4 Algorithm for Resistance Factor Calculation using Reliability Analysis

Despite the complexity of probabilistic slope stability analysis (which involves the generation of random fields; the location of the most critical slip surface and determination of the corresponding FS), the process of determination of the most probable ULS values of M_r , $M_{d,DL}$ and $M_{d,LL}$ can be divided into two major stages: (1) generation of a large number of M_r , $M_{d,DL}$ and $M_{d,LL}$ triples using Monte Carlo Simulation (MCS) such that the ratio of the number of triples that would lead to failure to the total number of triples is equal to the target probability of failure and (2) determination of the most probable ULS (design point) from the large number of instances of the triple (M_r , $M_{d,DL}$ and $M_{d,LL}$)

generated during the MCS using Advanced First-Order Reliability Analysis (AFORM) (14–16).

The following variables are treated as random variables: (1) soil unit weight γ , (2) apparent cohesion c (or undrained shear strength s_u), (3) friction angle ϕ , and (4) external live load q on the crest of slope. Slope geometry is taken as given. Pore pressure or groundwater pattern variability is not considered, which is consistent with the treatment of groundwater in design, which is deterministic and often conservative.

The algorithm consists of following steps:

- **Step 1:** Define the slope configuration to be analyzed. The slope geometry and location and thickness of layers are set. Initial values for the nominal values of c (s_u), ϕ , γ and q for each soil layer are also set.
- **Step 2:** Calculate the means of c_i (s_{ui}), ϕ_i , γ_i and q by multiplying the nominal values from Step 1 by their corresponding bias factors.
- **Step 3:** If q exists (i.e., $q \neq 0$), generate a random value for q using the calculated mean and coefficient of variation (COV).
- **Step 4:** Generate Gaussian random fields (GRF) for c_i (s_{ui}), ϕ_i and γ_i for each layer using the means of c_i (s_{ui}), ϕ_i and γ_i determined in Step 2 and the COVs of these parameters. In a Gaussian random field, the values of the corresponding quantity [c_i (s_{ui}), ϕ_i or γ_i] are different from point to point; but the expected value and the standard deviation of the quantity are the same at every point. A random realization of the slope follows from superposition of the random fields for the problem variables.
- **Step 5:** Perform a Simplified Bishop slope stability analysis and find the critical slip surface CSS (corresponding to the lowest FS) and the corresponding values of M_r , $M_{d,DL}$, and $M_{d,LL}$ for the specific random slope constructed in Step 4.
- **Step 6:** Store the calculated values of the resisting moment M_r and the driving moments ($M_{d,DL}$ and $M_{d,LL}$) for the CSS determined in Step 5 for later use.
- **Step 7:** Repeat Steps 3 through 6 to find the critical slip surface CSS and its corresponding factor of safety FS for each of N random realizations of the slope. N iterations of Steps 3 through 6 produce N values of FS . Count the cases for which $FS \leq 1$ (corresponding to “failure” or attainment of the ultimate limit state of the slope). Suppose there are n cases of failure; the P_f of the slope is then n/N .
- **Step 8:** Reconfigure the slope so as to achieve the target probability of failure. It is important to stress that the

present algorithm is not a design algorithm; rather its goal is to determine resistance factors for a slope with certain characteristics (fixed geometry, layering pattern and soil types). If the P_f calculated in Step 7 is not equal to or is not very close to the $P_{f,T}$, which is the probability of failure for which resistance and load factors are desired, go back to Step 1. If the probability of failure was too high, increase the initial nominal values of the soil strength parameters. Otherwise, decrease those values. Repeat Steps 1 through 7 until the calculated probability of failure P_f is acceptably close to the target probability of failure $P_{f,T}$. The number N of slope realizations is considered sufficient when the calculated P_f converges to within $\pm 5\%$ of the target probability of failure $P_{f,T}$ when it is equal to 0.01 or 0.001 and within $\pm 10\%$ of the target probability of failure $P_{f,T}$ when it is equal to 0.0001.

- **Step 9:** Determine the mean, COV and type of probability distribution for each of the moments M_r , $M_{d,DL}$, and $M_{d,LL}$ (the probability distribution type of each moment is determined by performing the Kolmogorov-Smirnov goodness-of-fit test), as well as the correlation coefficients between the three variables using all the resisting and driving moments generated from the MCSs.
- **Step 10:** Using the AFORM method, determine the most probable ultimate limit state (corresponding to the failure or design point discussed earlier).
- **Step 11:** Perform a conventional deterministic slope stability analysis using the nominal values of the soil parameters and external loads for which the calculated P_f is equal to the $P_{f,T}$. From this analysis, find the CSS and the corresponding nominal values of the M_r , $M_{d,DL}$, and $M_{d,LL}$. These are the values that an engineer performing a deterministic stability analysis of the slope would obtain.
- **Step 12:** Calculate the resistance and load factors using (1.4) and the most probable ULS (Design Point) moments obtained in Step 10 and nominal moments obtained in Step 11.

1.5 Calculation Example

In order to illustrate the 12-step algorithm for load and resistance factor determination, an example with COVs of c , ϕ , and γ equal to 0.4, 0.1, 0.1 and scale of fluctuation (s_f) values (which is the parameter that controls the degree of reduction in the correlation

coefficient between any two points when the distance between these two points increases) of 20 m with a target probability of failure $P_{f,T}$ of 0.01 and live uniform surcharge load ($q = 12 \text{ kN/m/m}$ and $\text{COV}_q = 0.205$) applied on the crest of a clay slope is now considered. Only undrained failure is assumed to be of concern. The slope has the geometry of Figure 1.2.

- **Step 1:** To find the combination of the nominal values of the soil parameters (s_u and γ) of each layer that produce the $P_{f,T}$ (0.01), the initial guess for the soil parameters was as follows: (1) layer 1: $s_{u1} = 20.0 \text{ kPa}$ and $\gamma_1 = 17.0 \text{ kN/m}^3$; (2) layer 2: $s_{u2} = 30.0 \text{ kPa}$ and $\gamma_2 = 18.0 \text{ kN/m}^3$; and (3) layer 3: $s_{u3} = 40.0 \text{ kPa}$ and $\gamma_3 = 18.5 \text{ kN/m}^3$. This constitutes Step 1 of the algorithm. Note that these initial guesses of the nominal values of soil parameters together with the slope geometry and layering could conceivably correspond to a real slope case. In that case, the probability of failure of that slope will almost certainly not be equal to the target probability of failure (0.01). So the nominal (and mean) values of the soil parameters will need to be adjusted in order to produce the desired probability of failure, as detailed subsequently.
- **Step 2:** Multiply the nominal values of s_u and γ of each layer and q ($=12 \text{ kN/m/m}$) by the corresponding bias factors (1.0 for s_u and γ ; 1.2 for q) to produce the mean value of each parameter.
- **Step 3:** Generate a random value of q .
- **Step 4:** Generate Gaussian random fields for each soil parameter, thereby defining a random realization of the slope.
- **Step 5:** Perform a slope stability analysis using the Bishop simplified method on the random realization of the slope generated in Step 4.
- **Step 6:** Store the driving and resisting moments corresponding to the most critical slip surface obtained in Step 5.
- **Step 7:** Repeat Steps 3 through 6 for N ($= 70,000$) times. The number of failure ($FS < 1$) cases was 456, so $P_f = 456/70000 = 0.0065$ for the given combination of soil parameter values.
- **Step 8:** As the initial assumed nominal values of soil parameters produce $P_f = 0.0065$, which is lower than $P_{f,T} = 0.01$, the nominal values of the soil parameters are iteratively adjusted until the combination of the adjusted parameters produce $P_f \approx 0.01$. In principle, the nominal values of the soil parameters could be varied in any manner to produce the $P_{f,T}$. However, it is preferable to retain the relative proportions of these values, so we

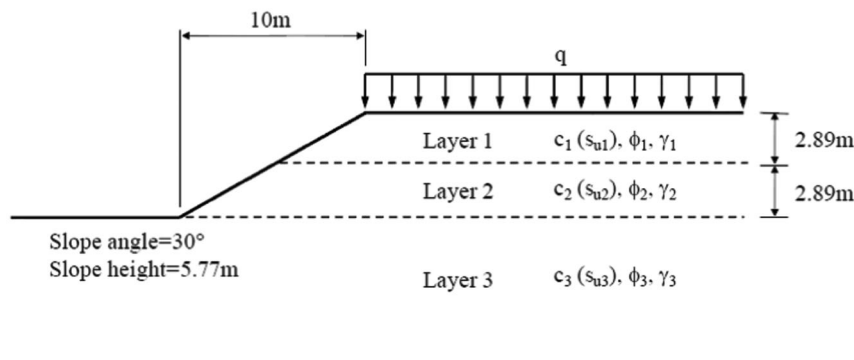


Figure 1.2 Geometry of a three-layer soil slope.

reduce the nominal values of initial s_{u1} , s_{u2} and s_{u3} proportionally until the calculated P_f becomes approximately equal to 0.01. The values of soil parameters producing $P_{f,T} \approx 0.01$ are as follows: (1) layer 1: $s_{u1} = 19.4$ kPa and $\gamma_1 = 17$ kN/m³; (2) layer 2: $s_{u2} = 29.1$ kPa and $\gamma_2 = 18.0$ kN/m³; and (3) layer 3: $s_{u3} = 38.8$ kPa and $\gamma_3 = 18.5$ kN/m³.

- **Step 9:** Due to the presence of external loads in this calculation example, there exist driving moments induced both by the self-weight of the soil ($M_{d,DL}$) and by the surcharge load on the crest of the slope ($M_{d,LL}$). The ULS surface is the locus of points corresponding to $FS = 1$ in the M_r - $M_{d,DL}$ - $M_{d,LL}$ three-dimensional space. Figure 1.3 shows the (M_r , $M_{d,DL}$, and $M_{d,LL}$) triples normalized with respect to the corresponding radius r_{slip} of the circular slip surface, so with axes M_r/r_{slip} , $M_{d,DL}/r_{slip}$ and $M_{d,LL}/r_{slip}$. The red points are failure points (i.e., points corresponding to $FS \leq 1.0$), and the plane is the ULS surface. For each of the three normalized moments (M_r/r_{slip} , $M_{d,DL}/r_{slip}$, and $M_{d,LL}/r_{slip}$), the mean, COV and distribution type, as well as the degree of correlation between the three, is then determined for use in Step 10. It is interesting to note, although not needed for the present calculations, that the distribution of the FS , shown in Figure 1.4, is approximately normal.
- **Step 10:** Using AFORM (essentially the application of the Rosenblatt transformation and Hohenbichler and Rackwitz procedure), determine the values of M_r/r_{slip} , $M_{d,DL}/r_{slip}$, and $M_{d,LL}/r_{slip}$ at the most probable ULS (i.e., at the design or failure point). These values are 753.130, 582.619, and 170.511 kNm/m/m, respectively.
- **Step 11:** Perform a conventional (deterministic) Bishop slope stability analysis using the nominal values of the soil parameters and given slope geometry to determine

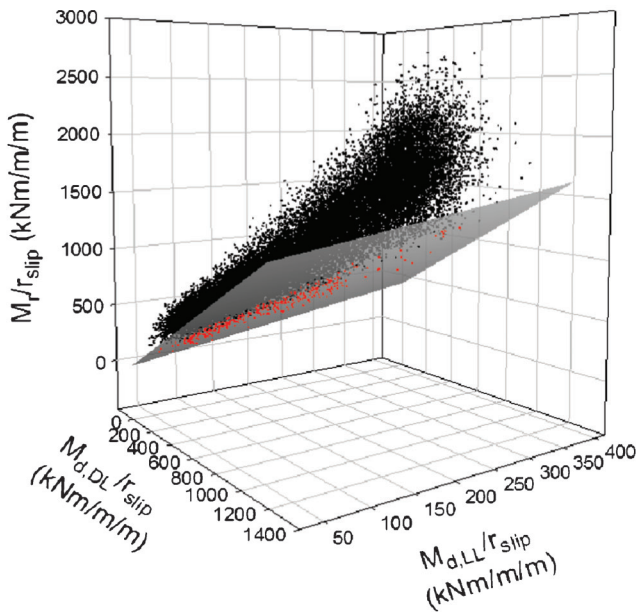


Figure 1.3 Scatter of driving moments $M_{d,DL}/r_{slip}$ and $M_{d,LL}/r_{slip}$ and resisting moment M_r/r_{slip} and the ULS surface (the grey plane is the ULS surface and the points below the ULS surface correspond to points with loading exceeding resistance).

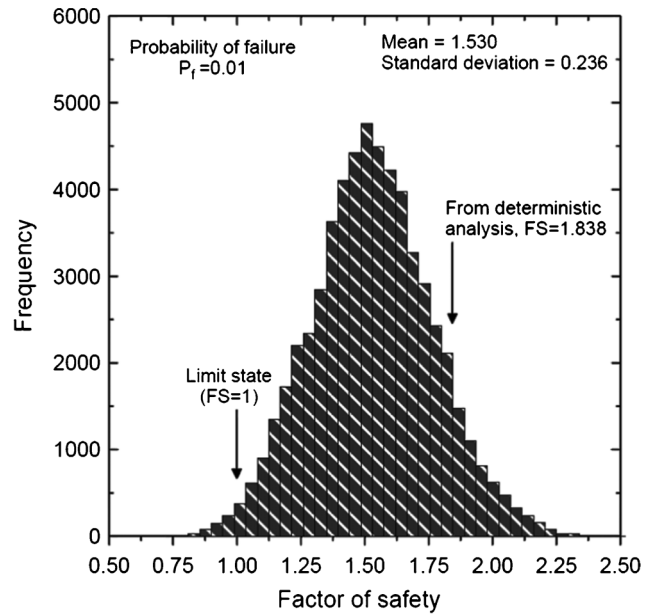


Figure 1.4 Distribution of FS value for the calculation example.

the nominal values of M_r , $M_{d,DL}$, and $M_{d,LL}$, which will be the values of these moments for the critical slip surface resulting from this analysis. The slope stability analysis produces an FS equal to 1.838 nominal values of M_r , $M_{d,DL}$, and $M_{d,LL}$ divided by the r_{slip} equal to 1300.662, 621.176, and 85.682 kNm/m/m, respectively.

- **Step 12:** The load and resistance factors follow from Equation (1.4): $RF = 0.579$, $(LF)_{DL} = 0.938$ and $(LF)_{LL} = 1.990$.

1.6 Case Studies

Generating sufficient sets of optimal load and resistance factors for different slope conditions is important for the determination of the load factors $(LF)_{DL}$ and $(LF)_{LL}$ and RF that are of general applicability. This is an expensive exercise, given the time required to perform the analyses, particularly for very low probabilities of failure. In this section, we use the 12-step procedure of the proposed algorithm to calculate load and resistance factors corresponding to three values of target probability of failure $P_{f,T}$: 0.0001, 0.001 and 0.01. Slopes with the same geometry as shown in Figure 1.5 are initially considered.

Assumed COV values for c (s_u), ϕ and γ are (0.4, 0.1, and 0.1) and (0.2, 0.05, and 0.05). The COV combination (0.4, 0.1, and 0.1) is expected to lead to slightly conservative factors. The isotropic scales of fluctuation of all soil parameters (c , ϕ , and γ) are taken as 20 m and 10 m, respectively, as discussed previously. Therefore, there are four COV- s_f combination cases. In case A, the COVs and s_f values of c , ϕ and γ are 0.4, 0.1, 0.1 and 20 m. The corresponding numbers for the other three cases are: 0.4, 0.1, 0.1 and 10 m (case B), 0.2, 0.05, 0.05 and 20 m (case C), and 0.2, 0.05, 0.05 and 10 m (case D).

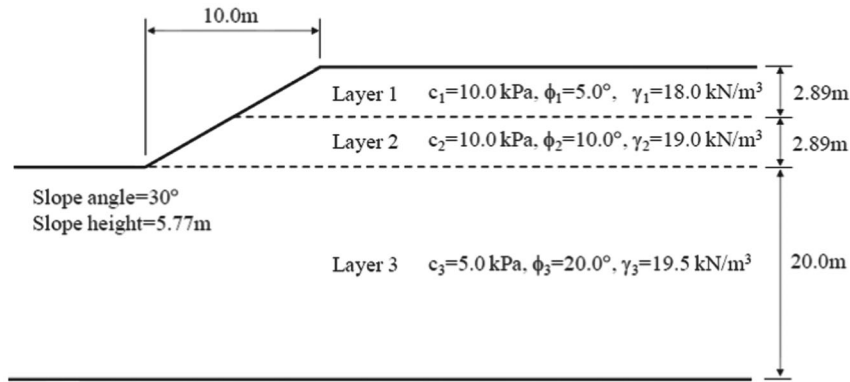


Figure 1.5 Geometry of a three-layer soil slope and initial values of its soil properties.

Cases B, C and D are discussed later. Readers will recognize the calculation example discussed previously as case A with $P_{f,T} = 0.01$ and a nonzero surcharge. Since calculations are done for three values of target probability of failure and the surcharge takes a value of either zero or 12 kN/m², there are a total of six calculation cases corresponding to case A.

Six additional calculation cases are constructed from the same geometry by now expressing strength in terms of an undrained shear strength. The results of these twelve calculation cases (with COV and s_f values for c (s_u), ϕ and γ of 0.4, 0.1, 0.1 and 20m, respectively, $P_{f,T}$ equal to 0.01, 0.001 or 0.0001, and q equal to 0 or 12 kN/m²) are summarized in Table 1.2. The table shows the final nominal values of c (s_u), ϕ , and γ producing the $P_{f,T}$ and the corresponding load and resistance factors. Table 1.2 shows the resistance factors that should be used if a different pair of load factors, identified in the table as “proposed” load factors, is used in design.

It is clear from Table 1.2 that the resistance and load factor values obtained in calculation cases 1, 3 and 5 are

quite different from those calculated in cases 2, 4 and 6, respectively, which differ from 1, 3 and 5 only in that a surcharge is applied. This is not a surprise, as the connection between load and resistance factors and the presence of live loads has been shown to quite significant in other studies (e.g., Basu and Salgado (1)). For a given $P_{f,T}$, the factor values calculated for undrained slopes (cases 1 to 6) are also fairly different from those obtained from drained slopes (cases 7 to 12).

1.7 Application to Design Code Development

The RF and the LFs resulting from calculations following Steps 1-12 are not independent. Load factors are connected to a specific resistance factor, as shown by the results of the calculation cases considered earlier and summarized in Table 1.2. However, design codes usually specify values of load factors to use in design. If resistance and load factors are determined as done in the present study, the load factor will not match the code-specified load factor. In order to use the results of

TABLE 1.2

Nominal values of c (s_u), ϕ , γ and the corresponding resistance and load factors, equivalent factor of safety, and the adjusted resistance factors for load factors $LF_{DL}^* = 1.0$ and $LF_{LL}^* = 1.55$ for three target probabilities of failure and the slope of Figure 1.5 subject to a surcharge of zero or 12 kN/m/m.

Analysis	Case	$P_{f,T}$	q	Layer 1			Layer 2			Layer 3			Factors from the Analyses			RF^* and FS^{eq} for $LF_{DL}^* = 1.0$ and $LF_{LL}^* = 1.55$	
				c (s_u)	ϕ	γ	c (s_u)	ϕ	γ	c (s_u)	ϕ	γ	LF_{DL}	LF_{LL}	RF	FS^{eq}	RF^*
Undrained	1	0.01	12	19.4	—	17	29.1	—	18	38.8	—	18.5	0.94	1.99	0.58	1.84	0.57
	2	—	—	15.8	—	—	23.7	—	—	31.6	—	—	0.97	—	0.57	1.70	0.58
	3	0.001	12	22.3	—	—	33.5	—	—	44.7	—	—	0.95	1.98	0.51	2.12	0.50
	4	—	—	18.6	—	—	28.0	—	—	37.3	—	—	0.96	—	0.48	2.01	0.49
	5	0.0001	12	24.5	—	—	36.8	—	—	49.1	—	—	0.94	1.97	0.46	2.33	0.45
	6	—	—	21.1	—	—	31.6	—	—	42.1	—	—	0.96	—	0.42	2.27	0.44
Drained	7	0.01	12	10.3	10.3	18	5.1	20.5	19	7.2	20.5	19.5	0.73	0.97	0.60	1.27	0.83
	8	—	—	9.2	9.2	—	4.6	18.4	—	6.4	18.4	—	0.95	—	0.80	1.19	0.83
	9	0.001	12	11.0	11.0	—	5.5	22.0	—	7.7	22.0	—	0.79	0.92	0.60	1.30	0.78
	10	—	—	9.9	9.9	—	4.9	19.7	—	6.9	19.7	—	0.81	—	0.64	1.28	0.78
	11	0.0001	12	11.6	11.6	—	5.8	23.3	—	8.1	23.3	—	0.61	0.75	0.43	1.45	0.73
	12	—	—	10.5	10.5	—	5.3	21.0	—	7.4	21.0	—	0.69	—	0.50	1.38	0.72

Units: q (kN/m), c or s_u (kPa), ϕ (degrees), and γ (kN/m³).

the analysis described here with code-prescribed load factors, the resistance factor must be adjusted. We can make use of inequality (1.2) to make this adjustment.

Inequality (1.2), at the limit of equality, is expressed as

$$(RF^*) M_r|_n = (LF_{DL}^*) M_{d,DL}|_n + (LF_{LL}^*) M_{d,LL}|_n \quad (1.7)$$

for load and resistance factors as prescribed in a code (indicated throughout this report by the superscripted asterisk) and as

$$(RF) M_r|_n = (LF_{DL}) M_{d,DL}|_n + (LF_{LL}) M_{d,LL}|_n \quad (1.8)$$

for load and resistance factors determined following Steps 1 through 12 of the algorithm presented earlier. Combining both equations, we can determine the value of the adjusted resistance factor that matches any code-prescribed load factors:

$$RF^* = RF \frac{(LF_{DL}^*) (M_{d,DL}|_n) + (LF_{LL}^*) (M_{d,LL}|_n)}{(LF_{DL}) (M_{d,DL}|_n) + (LF_{LL}) (M_{d,LL}|_n)} \quad (1.9)$$

The current AASHTO LRFD bridge design specifications (17) use an RF that is equal to the inverse of the traditional values of FS because it assumes all the LFs for different types of loads associated with slope designs to be equal to one. The Eurocode (EN-1997) does prescribe a factor on variable action of 1.3, but use of Eurocode prescriptions for slope stability is still debated (e.g., Lansivara and Poutanen (18)). Therefore, in connection with slope stability, which values of load factors to prescribe is still somewhat of an open question. A possible way to determine appropriate LFs for undrained analysis of slopes made of Tresca soils (frictionless soils with strength equal to s_u) and drained analysis of slopes made of soils modeled as Mohr-Coulomb ($c-\phi$) materials is to require that all the LFs for DLs and LLs be greater than or equal to one ($LF \geq 1$) and then look for the combination of LFs that results in the narrowest range of RF values for each of the three different $P_{f,T}$ values (0.0001, 0.001 and 0.01). The dead load and live load factors obtained in this manner for the 12 cases corresponding to set A and summarized in Table 1.2 are 1.0 and 1.5 for undrained analyses and 1.0 and 1.55 for drained analysis of slopes. For simplicity, a $LF_{LL}^* = 1.55$ is assumed for both undrained and drained slope stability analyses.

Using these LF^* values, the corresponding RF^* values are summarized in Table 1.2. For each case, the corresponding FS values obtained from deterministic analyses are also provided in Table 1.2. The results in Table 1.2 show that, when appropriate LF^* values are selected, the RF^* for each $P_{f,T}$ varies within a relatively narrow range. For example, RF^* for $P_{f,T} = 0.01$ is 0.57 – 0.58 for undrained and 0.83 for drained analysis of slopes.

1.8 Degree of Conservatism of Results

For sufficiently low probability of failure, factors of safety resulting from calculations for variability set A

are slightly lower than the commonly used $FS = 1.5$ for drained analysis but are more than slightly greater than 1.5 for undrained analysis of clay slopes. Although the assumptions made in this study for random fields in clay may be overly conservative, higher probabilities of failure may be implicit in analyses done for clay slopes with $FS = 1.5$. Lansivara and Poutanen (18), for example, suggest that there is an “overestimation of safety” implied in typical factors of safety used in total stress analysis of the stability of clay slopes. The results of analyses of sets B, C and D, discussed earlier, allow assessment of the degree of conservatism resulting from the values of COV and scale of fluctuation assumed for the set A conditions considered earlier and summarized in Table 1.2.

Resistance and load factors for undrained and drained slope stability analysis are determined for sets B, C, and D of scale of fluctuation and COVs of soil parameters following the same procedure as for set A. The choice of load factors for DLs and LLs that resulted in the narrowest range of RF^* values for each of the three different $P_{f,T}$ values (0.0001, 0.001 and 0.01) for variability sets A through D, therefore spanning a wide range of soil variability parameters, were $LF_{DL}^* = 1.0$ and $LF_{LL}^* = 1.19$ for undrained analyses and $LF_{DL}^* = 1.0$ and $LF_{LL}^* = 1.20$ for drained analyses, respectively. Since simplicity is desired in design prescriptions, $LF_{DL}^* = 1.0$ and $LF_{LL}^* = 1.2$, which should work well for the range of variability spanned by variability sets A-D, are proposed for slope stability checks.

Resistance factors compatible with $LF_{DL}^* = 1.0$ and $LF_{LL}^* = 1.2$ and equivalent safety factors for the less conservative combinations of coefficients of variation and scales of fluctuation associated with sets B, C and D are given in Table 1.3. The RF^* values and FS^{eq} for set A (most conservative) increased on average by 33% and decreased on average by 28%, respectively, if the COVs and s_f values of c (s_u), ϕ and γ for set A are all reduced by half, leading to values of the COVs and scale of fluctuation corresponding to set D. The FS^{eq} range corresponding to $P_{f,T}$ from 0.0001 to 0.01 for the 12 examples for the combinations of coefficients of variation and scales of fluctuation of set D was 1.053-1.442, which are all less than the commonly-used $FS = 1.5$. The results from sets A and D are very likely to bound the values of resistance and load factors for most slope stability problems to be found in practice. More research is needed on precise definition of values of both the scale of fluctuation and the coefficient of variation of each pertinent soil property so that final values of resistance and load factors that may be used for a range of slope stability problems can be determined.

A possible way in which a designer can use the results summarized in Table 1.3 is for the designer to estimate the variability of the soils in the slope and select the appropriate resistance factor from one of sets A through D. In so doing, it is desirable to keep in mind that set A is probably conservative for total stress analysis of clay slopes.

TABLE 1.3

Resistance factors and equivalent factor of safety values for different combinations (sets A to D) of COV values and scales of fluctuation of c (s_u), ϕ , and γ corresponding to load factors $LF_{DL}^* = 1.0$ and $LF_{LL}^* = 1.2$

Calculation Case	$P_{f,T}$	q (kN/m)	RF^*				FS^{eq}				
			set A	set B	set C	set D	set A	set B	set C	set D	
Undrained analyses	1	0.01	12	0.55	0.60	0.73	0.76	1.840	1.684	1.397	1.339
	2	—	—	0.58	0.63	0.81	0.83	1.702	1.580	1.232	1.203
	3	0.001	12	0.48	0.54	0.68	0.73	2.119	1.893	1.489	1.399
	4	—	—	0.49	0.56	0.76	0.79	2.009	1.776	1.314	1.264
	5	0.0001	12	0.44	0.48	0.64	0.71	2.327	2.100	1.581	1.442
	6	—	—	0.44	0.50	0.71	0.76	2.269	1.973	1.397	1.307
Drained analyses	7	0.01	12	0.80	0.86	0.92	0.93	1.267	1.173	1.106	1.092
	8	—	—	0.83	0.87	0.94	0.95	1.191	1.142	1.062	1.053
	9	0.001	12	0.75	0.81	0.89	0.90	1.300	1.258	1.144	1.132
	10	—	—	0.78	0.81	0.89	0.92	1.275	1.222	1.113	1.076
	11	0.0001	12	0.70	0.78	0.86	0.87	1.447	1.302	1.181	1.170
	12	—	—	0.72	0.78	0.86	0.90	1.377	1.279	1.150	1.100

Set A: $COV_{c(su)} = 0.4$; $COV_{\phi} = 0.1$; $COV_{\gamma} = 0.1$; $s_f = 20$ m.

Set B: $COV_{c(su)} = 0.4$; $COV_{\phi} = 0.1$; $COV_{\gamma} = 0.1$; $s_f = 10$ m.

Set C: $COV_{c(su)} = 0.2$; $COV_{\phi} = 0.05$; $COV_{\gamma} = 0.05$; $s_f = 20$ m.

Set D: $COV_{c(su)} = 0.2$; $COV_{\phi} = 0.05$; $COV_{\gamma} = 0.05$; $s_f = 10$ m.

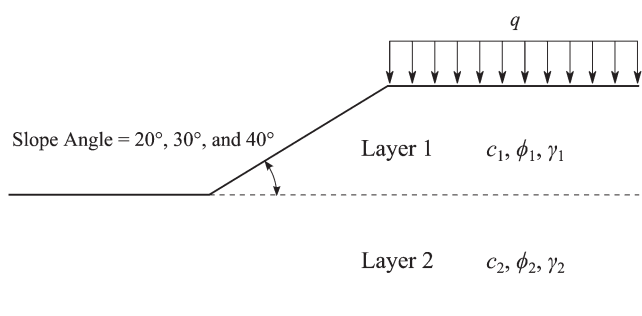


Figure 1.6 Geometry of a two-layer soil slope with different slope angles (used for undrained slope cases only).

1.9 Impact of Geometry

In order to assess the impact of geometry on the resistance and load factors, additional resistance factor calculations were performed by varying slope angle and

soil layering as a check on values reported so far. A two-layer undrained soil slope with slope angles of 20° , 30° , and 40° (Figure 1.6) is assumed to examine the effect of slope geometry on the resistance factors for set D ($COV_{c(su)} = 0.2$; $COV_{\phi} = 0.05$; $COV_{\gamma} = 0.05$; $s_f = 10$ m). The proposed load factors $LF_{DL}^* = 1.0$ and $LF_{LL}^* = 1.2$ were used in the resistance factor calculation.

For each of the two target probabilities of failure considered ($P_{f,T} = 0.01$ and 0.001), the difference in resistance factor between different slope geometries was insignificant for case D as shown in Table 1.4 where the RF^* values compatible with $LF_{DL}^* = 1.0$ and $LF_{LL}^* = 1.2$ increase only slightly with increasing slope angle.

It is apparent that, when realistic values of COV and scale of fluctuation of the soil properties are assumed (values close to those of set D), the resulting RF^* values do not depend strongly on slope geometry, suggesting that rigorous reliability analysis algorithm proposed in the present study can be used effectively to produce load and resistance factors for use in design.

TABLE 1.4

Comparison between resistance factors and equivalent factor of safety values for combination sets D ($COV_{c(su)} = 0.2$; $COV_{\gamma} = 0.05$; $s_f = 10$ m) for the proposed $LF_{DL}^* = 1.0$ and $LF_{LL}^* = 1.2$ for different slope geometries and soil layer conditions (for undrained slope analyses)

Slope angle	$P_{f,T}$	Nominal values (k Nm/m)			LF and RF			RF^* and FS^{eq} for LF^*	
		$M_{d,DL}$	$M_{d,LL}$	M_r	LF_{DL}	LF_{LL}	RF	RF^*	FS^{eq}
20°	0.01	248.7	66.3	463.4	0.814	1.973	0.719	0.70	1.47
	0.001	249.0	66.5	492.6	0.652	1.656	0.553	0.66	1.56
30°	0.01	621.8	85.5	947.1	0.616	1.358	0.527	0.76	1.34
	0.001	622.1	85.6	989.5	0.482	1.195	0.406	0.73	1.40
40°	0.01	213.8	41.9	337.5	1.867	3.258	1.587	0.78	1.32
	0.001	215.5	42.5	359.1	1.803	3.196	1.460	0.74	1.39

2. FURTHER VALIDATION IMPLEMENTATION OF RESISTANCE AND LOAD FACTORS

2.1 Implementation

As shown in the previous chapter, the load factors LF^* of 1.0 for dead load and 1.2 for live load were proposed for undrained stability analysis of slopes. According to Table 1.3, resistance factor RF^* under undrained conditions for the proposed load factors is in the range of 0.73 to 0.83, 0.68 to 0.79, and 0.64 to 0.76 for target failure probability $P_{f,T}$ values of 0.01 (1%), 0.001 (0.1%), and 0.0001 (0.01%), respectively, with slightly conservative estimates of spatial variability of soil properties (sets C and D in Table 1.3). From the range of calculated resistance factors, the RF^* s of 0.75, 0.70, and 0.65 can be adopted for $P_{f,T}$ of 0.01, 0.001, and 0.0001, respectively. The resistance factors used in this report are summarized in Table 2.1.

This report examines a total of six slopes (cases A through F) provided by INDOT. The cross-section views of the slope in each case are illustrated in Figure 2.1 through Figure 2.6. The soil profile for each case is summarized in Table 2.2. In cases A and B, the weak clay layer below the slope was removed and a sand layer assumed in its place to reinforce the slope. In cases D and E, there is a relatively thick soft clay layer, therefore the FS s in these cases are expected to be lower than in other cases. For all cases, the short-term (undrained) properties (c for clay and ϕ for sand) of soil are provided. To analyze short-term stability of these slopes, the proposed undrained load and resistance factors were used in the analyses.

Figure 2.7 illustrates the geometry parameters of the target slopes in the analysis. The slope length L_s and height H_s are defined in terms of the horizontal and vertical distances from the toe to the crest of the slope. The angle of the slope θ_s can be defined mathematically as $\tan^{-1}(H_s/L_s)$. L_q is the width of the zone over which live load q is applied. L_m is the horizontal distance from the center of the live load to the center of the (circular) critical slip surface. Using these definitions, these parameters for the geometry of each of the six slopes are listed in Table 2.3. The angle of the slope is between 14 and 20 degrees. Case A has the largest slope angle, and Case B has the smallest slope angle.

Since the proposed load factors for dead and live loads are different (1 and 1.2, respectively), the contributions of dead and live loads to the total load (driving moment) need to be considered separately. This requires that the driving moments due to dead and

live loads be supplied by the slope stability software separately. Alternatively, it is possible to separate the components of the driving moment if the coordinates of the center of the critical slip surface (assumed here as circular) is known. Once the slip surface is defined, using the center coordinates of a slip surface, the driving moment ($M_{d,LL}$) mobilized by the live load can be calculated as:

$$M_{d,LL} = qL_qL_m \quad (2.1)$$

The driving moment from the dead load ($M_{d,DL}$) can be calculated by subtracting the driving moment caused by the live load ($M_{d,LL}$) from the total driving moment (M_d).

The results of the original STABL analyses performed by INDOT, as provided to us, did not have the moments supplied separately or the slip surface center coordinates; the cases were re-analyzed using both STABL and Geostudio 2007®. As shown in Table 2.4, there is no significant difference between FS s from STABL® and Geostudio 2007®.

In the next step, the resistance factor and load factors were applied to the resistance moment M_r , the driving moment $M_{d,DL}$ due to dead loads and the driving moment $M_{d,LL}$ due to live loads. The factored resistance moment M_{rf} ($= RF \cdot M_r$) and the factored driving moment M_{df} ($= \sum LF \cdot M_d$) were used to determine whether the failure probability is less or greater than the target failure probability.

2.2 Results

If the factored resistance moment M_{rf} is greater than the factored driving moment M_{df} , the probability of failure P_f of the slope is greater than the target probability of failure $P_{f,T}$ assumed. Otherwise, the failure probability of the slope is less than $P_{f,T}$. To quantify this, the ratio R_f ($= M_{rf}/M_{df}$) is estimated for each case; if $R_f \geq 1$, P_f is less than $P_{f,T}$, whereas P_f is greater than $P_{f,T}$ if $R_f < 1$. It should be noted that $R_f < 1$ does not mean a slope is unstable; it means that the probability of failure of the slope is less than the target failure probability $P_{f,T}$.

Table 2.5 lists the resisting moment M_r , the factored resisting moment M_{rf} , the driving moment $M_{d,DL}$ caused by the dead load, the driving moment $M_{d,LL}$ from the live load, the factored driving moment M_{df} , the ratio R_f and FS for each case when the target probability of failure $P_{f,T}$ is 0.01 (1%). For all cases, the ratio R_f is greater than one and the failure probability P_f is less than the target probability of failure $P_{f,T}$ ($= 1\%$). Figure 2.8 shows the strong linear relationship between the ratio R_f and FS . Once the regression line between R_f and FS is found, FS corresponding to $R_f = 1.0$, for which the failure probability is equal to the prescribed target probability of failure, is set as the minimum required factor of safety FS_{req} . If FS is less than FS_{req} , the failure probability P_f is greater than the target failure probability $P_{f,T}$; otherwise, P_f is less than $P_{f,T}$. Figure 2.8 shows that FS_{req} for 1% failure

TABLE 2.1
Range and selected values of adjusted resistance factors RF^* for the proposed load factors ($LF^*_{DL} = 1.0$ and $LF^*_{LL} = 1.2$) with respect to the failure probability $P_{f,T}$

$P_{f,T}$	Range of RF^*	RF^* used
0.01 (1%)	0.73 to 0.83	0.75
0.001 (0.1%)	0.68 to 0.79	0.70
0.0001 (0.01%)	0.64 to 0.76	0.65

INDOT US 31 Kokomo Bypass Contract 3 Bridge Over US31 Transverse Section ST

n:\projects\2008\1085184\analyses\stabl\brovus31_4004+50_tr_st.pl2 Run By: H.C. Nutting 9/11/2008 02:46PM (w/ UNDERCUT)

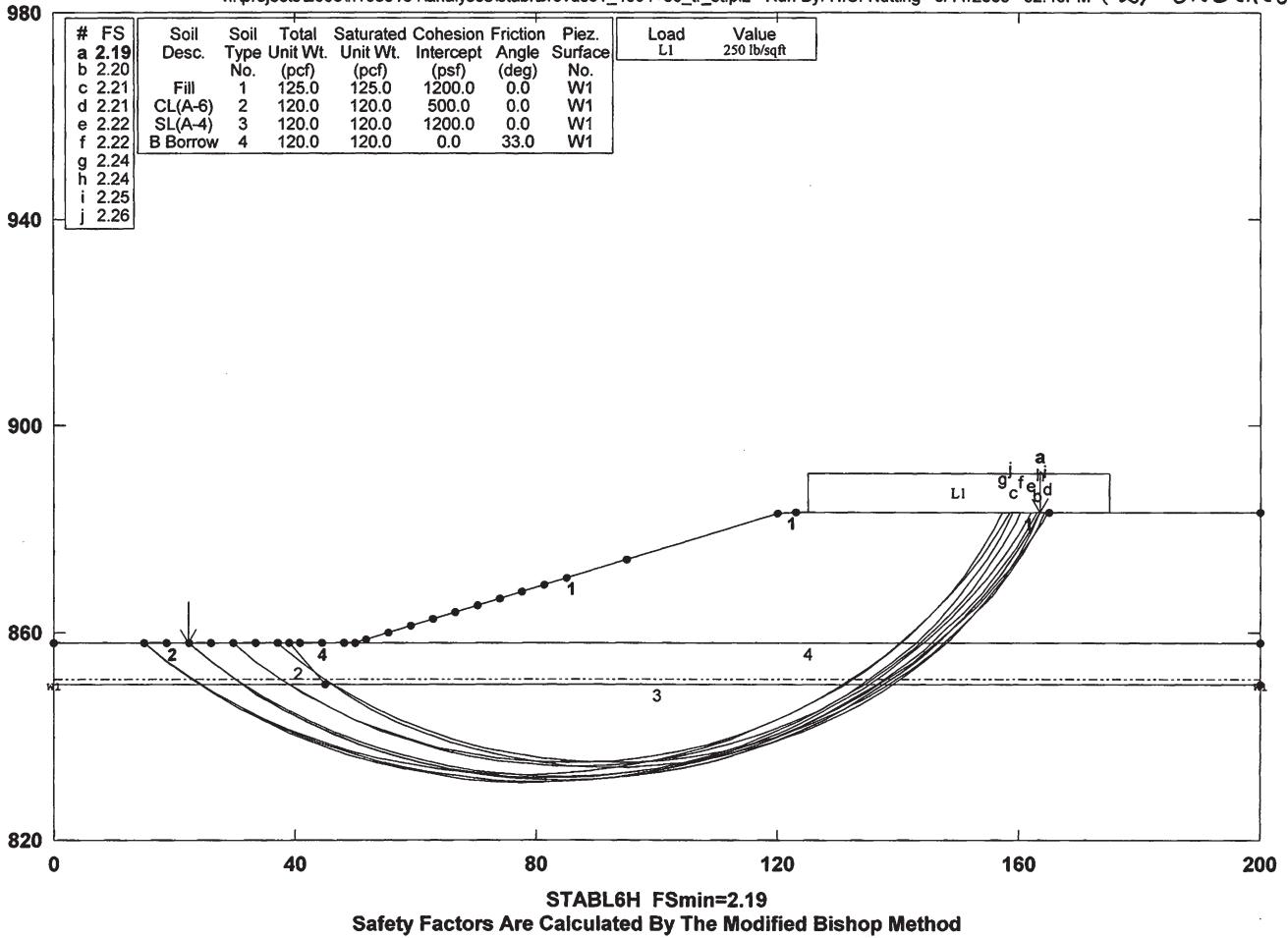


Figure 2.1 Cross-section view of the slope in case A.

INDOT US 31 Kokomo Bypass Contract 3 Bridge Over Kokomo Cr. Trans. Sec. ST

n:\projects\2008\1085184\analyses\stabl\brovkokomock_1269+50_tr_st_uc.pl2 Run By: H.C. Nutting 9/11/2008 03:14PM (J) UNDERCUT

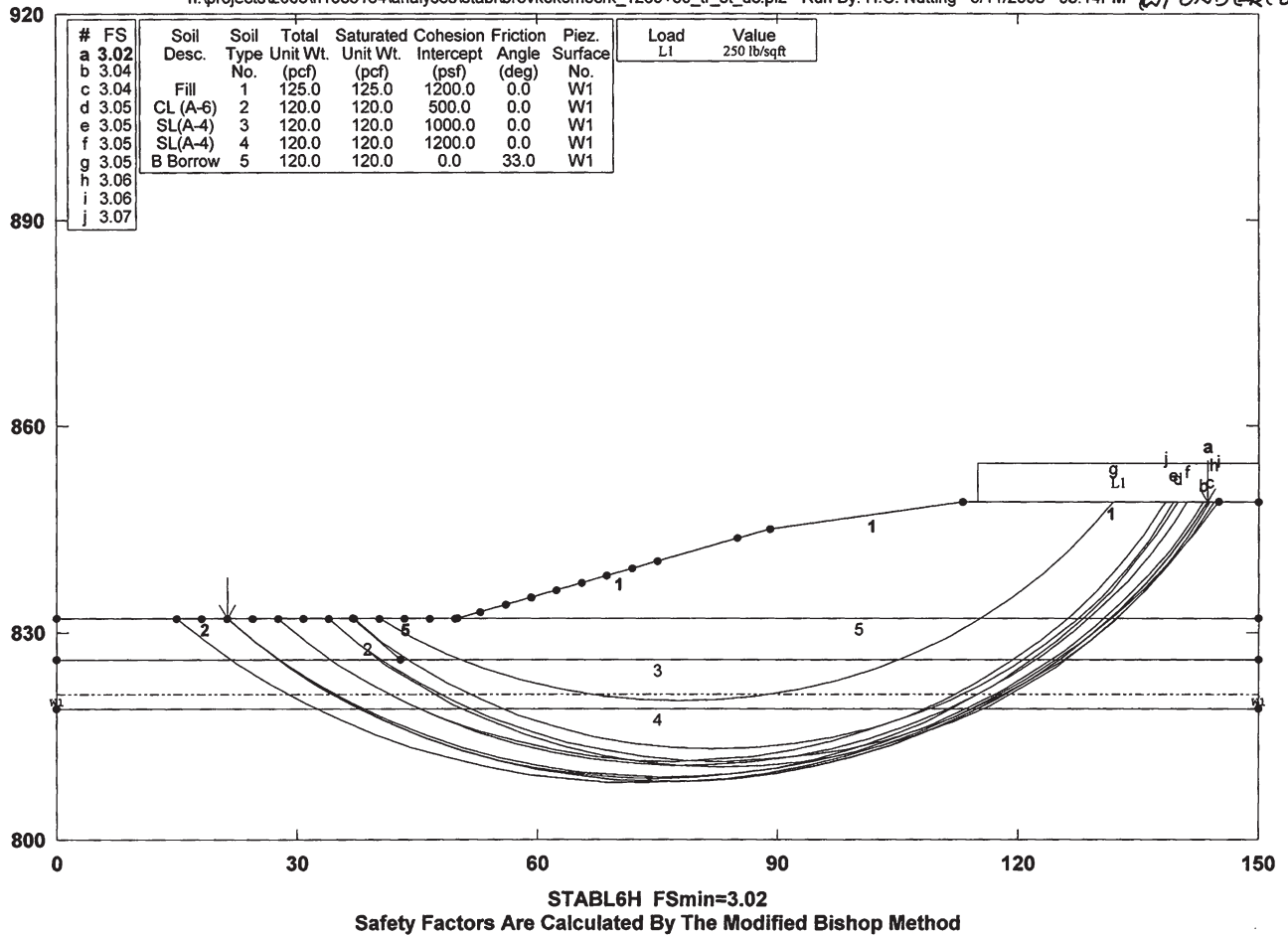


Figure 2.2 Cross-section view of the slope in case B.

INDOT US 31 Kokomo Bypass Contract 3 Stability @ Sta. 1982+50 Ramp C ST

n:\projects\2008\1085184\analyses\stabl\sta.1982+50_rampc_st.pl2 Run By: H.C. Nutting 9/11/2008 09:49AM

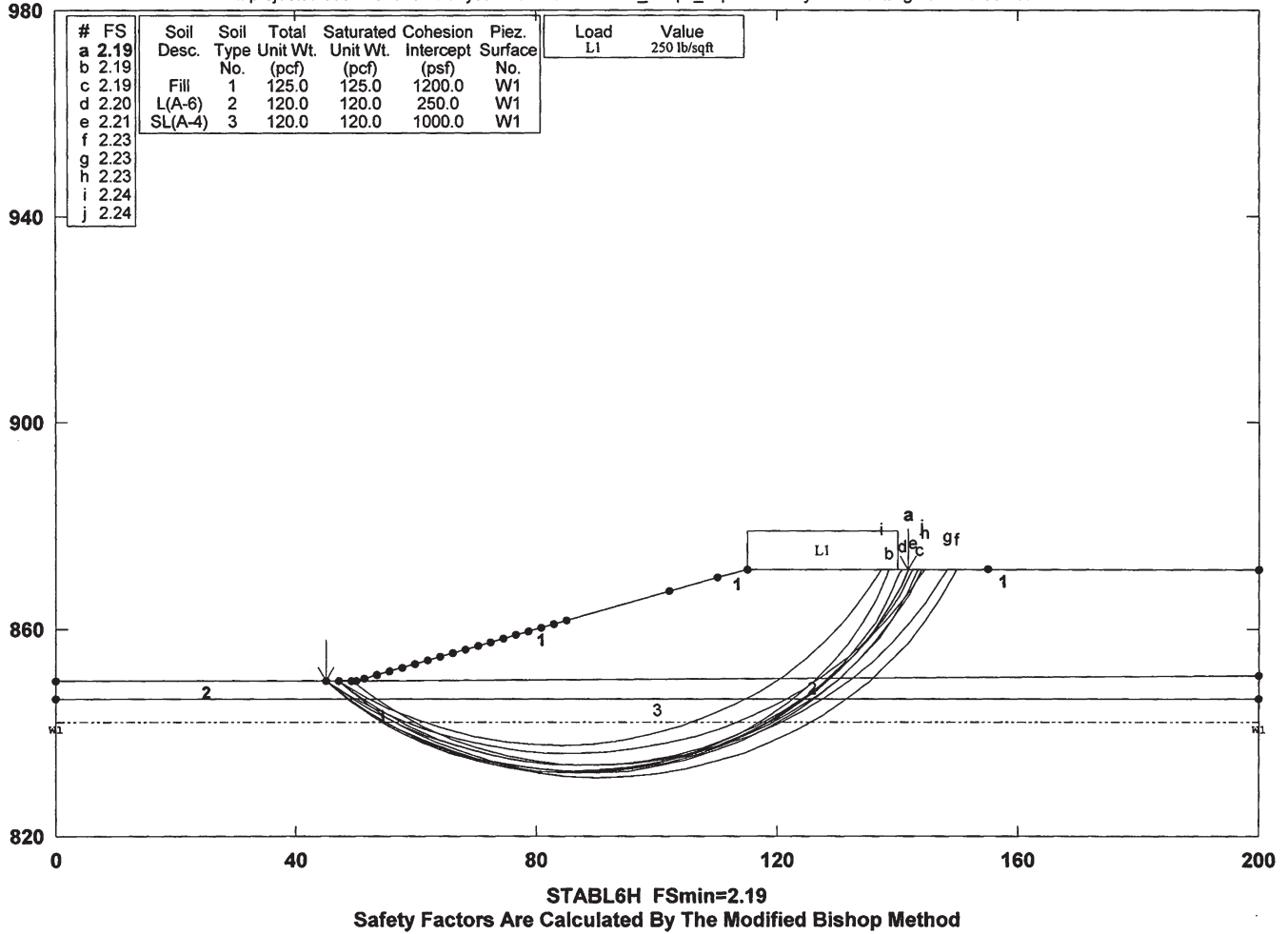


Figure 2.3 Cross-section view of the slope in case C.

INDOT US 31 Kokomo Bypass Contract 3 Stability @ Sta. 1236+00 Line A ST

n:\projects\2008\1085184\analysis\stabl\sta.1236+00_linea_st.pl2 Run By: H.C. Nutting 9/11/2008 10:31AM

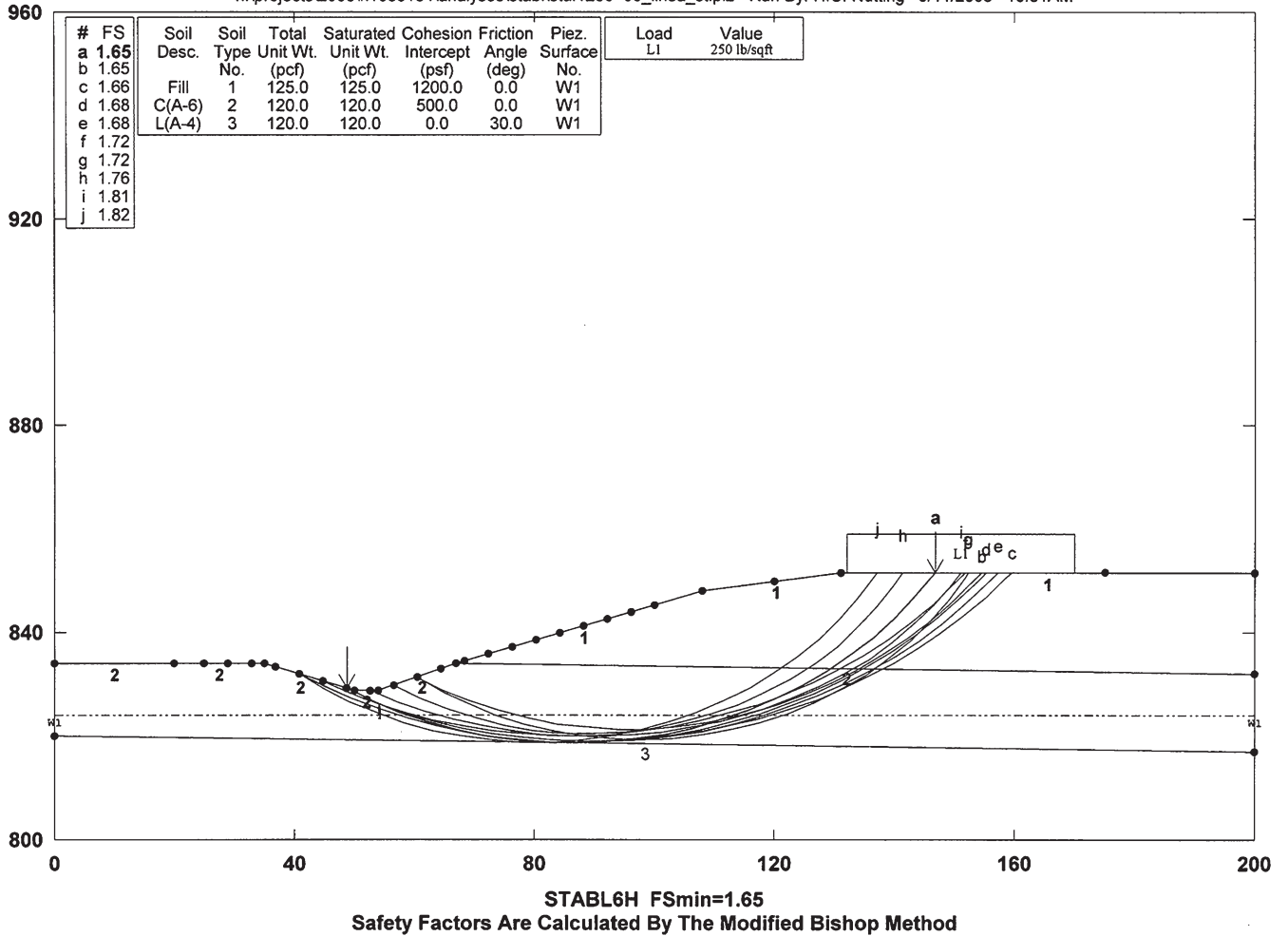


Figure 2.4 Cross-section view of the slope in case D.

INDOT US 31 Kokomo Bypass Contract 3 Stability @ Sta. 2231+00 Ramp D ST

n:\projects\2008\1085184\analyses\stablsta.2231+00_rampd_st.pl2 Run By: H.C. Nutting 9/11/2008 09:21AM

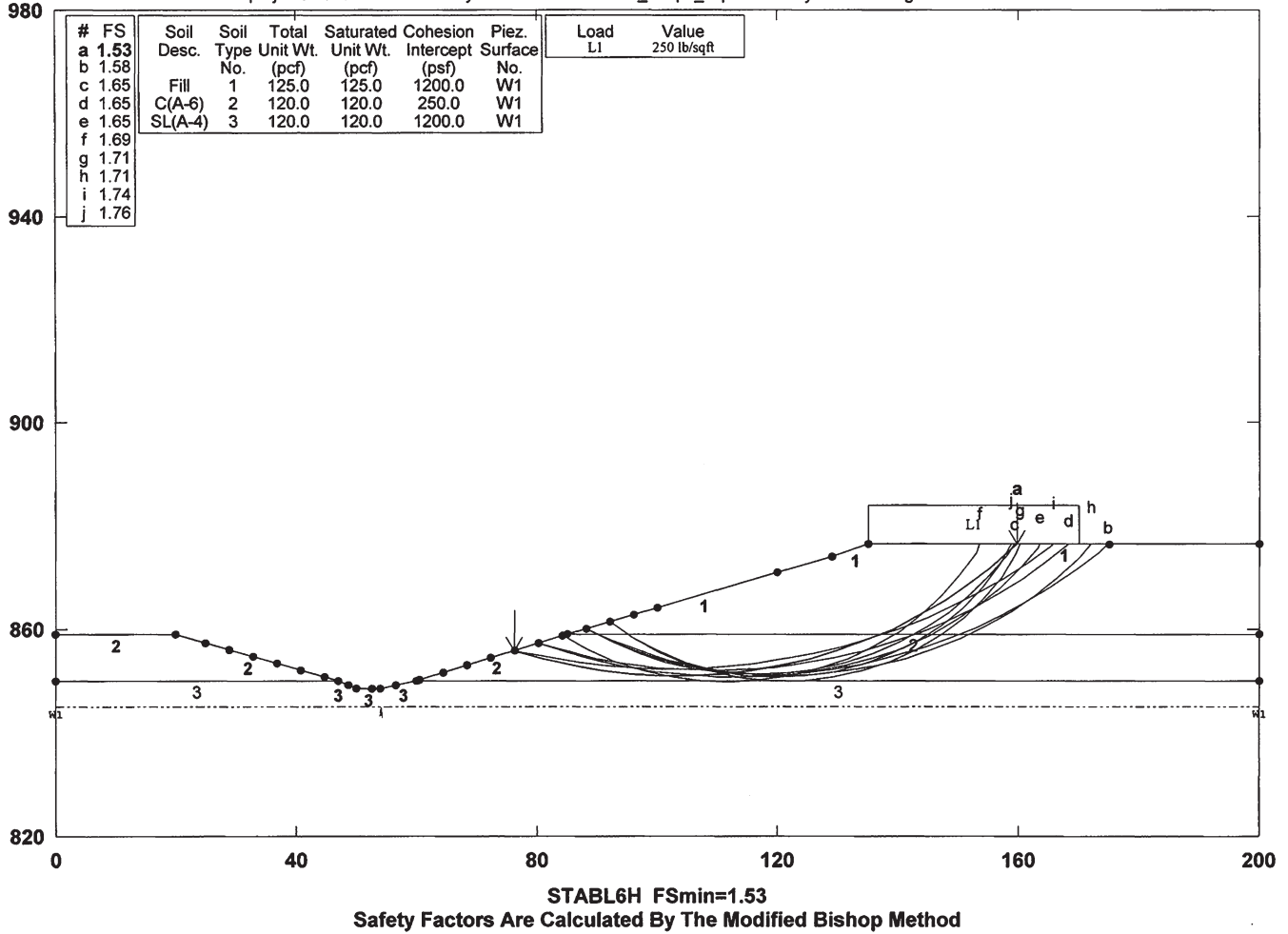


Figure 2.5 Cross-section view of the slope in case E.

INDOT US 31 Kokomo Bypass Contract 3 Bridge Over Kokomo Cr. Trans. Sec. ST

n:\projects\2008\1085184\analyses\stabil\brovkokomocrk_1269+50_tr_st.pl2 Run By: H.C. Nutting 9/11/2008 03:19PM (W/O UNDERCUT)

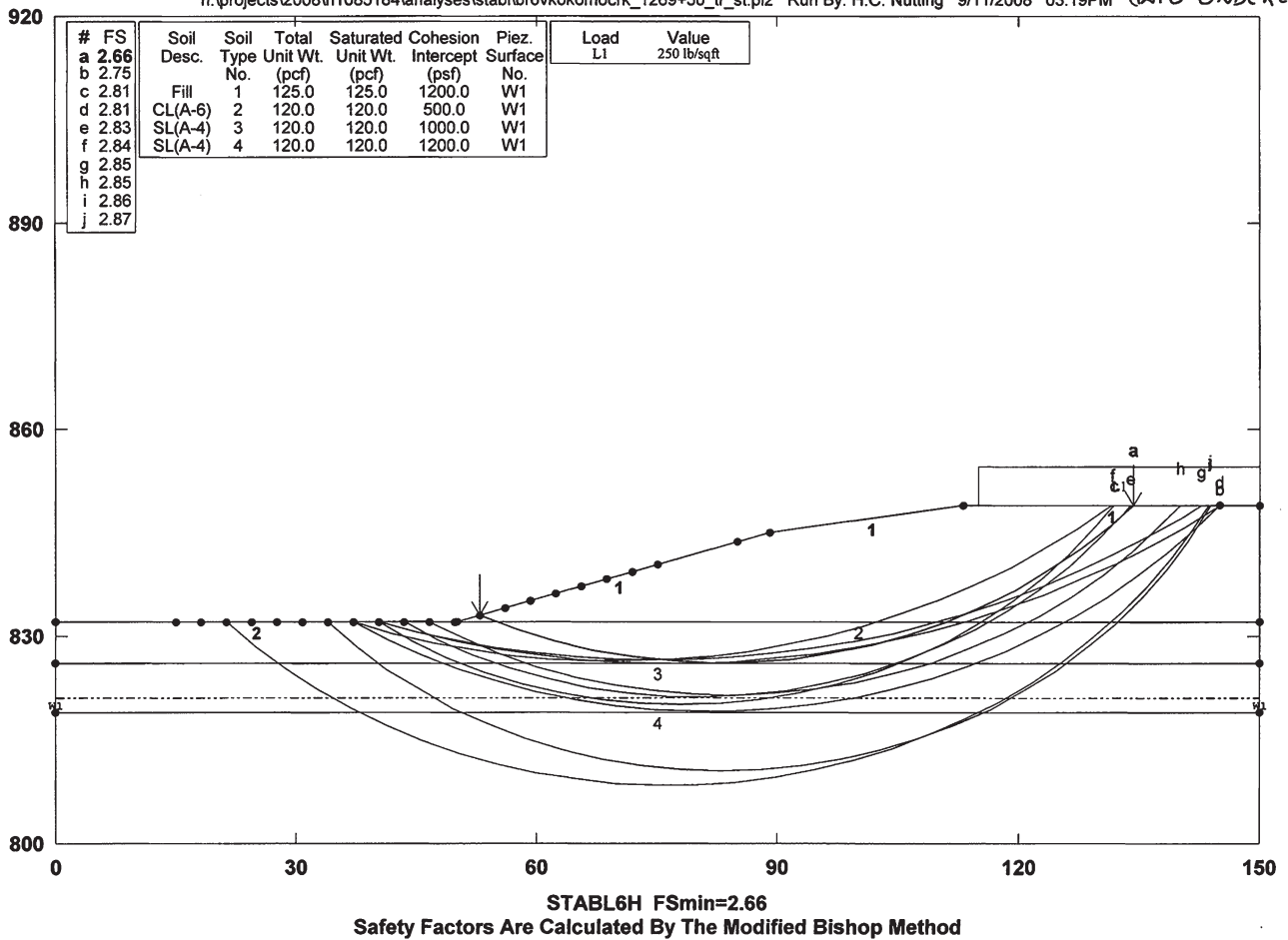


Figure 2.6 Cross-section view of the slope in case F.

TABLE 2.2
Soil profile for each case

Case	Layer No.	γ (pcf)	c (psf)	ϕ (deg)	Top elevation (ft)	Thickness (ft)	Description
A	1	125	1200	—	883.0	25.0	Fill
	2	120	500	—	858.0	8.0	CL (A-6), WT at 851'
	3	120	—	33	858.0	8.0	B Borrow (below the slope), WT at 851'
	4	120	1200	—	850.0	—	CL (A-4)
B	1	125	1200	—	848.8	16.5	Fill
	2	120	500	—	832.3	6.0	CL (A-6)
	3	120	—	33	832.3	6.0	B Borrow (below the slope)
	4	120	1000	—	826.3	7.5	SL (A-4), WT at 821'
	5	120	1200	—	818.8	—	SL (A-4)
C	1	125	1200	—	871.1	20.5	Fill
	2	120	250	—	850.6	4.2	L (A-6)
	3	120	1000	—	846.6	—	SL (A-4), WT at 841.1'
D	1	125	1200	—	852.6	20	Fill
	2	120	500	—	832.6	15.8	C (A-6), WT at 824.2'
	3	120	—	30	816.8	—	L (A-4)
E	1	125	1200	—	871.2	17.4	Fill
	2	120	250	—	853.8	8.2	C (A-6)
	3	120	1200	—	845.6	—	SL (A-4), WT at 840.5'
F	1	125	1200	—	849.0	17.0	Fill
	2	120	500	—	832.0	6.0	CL (A-6)
	3	120	1000	—	826.0	8.0	SL (A-4), WT at 821.0'
	4	120	1200	—	818.0	—	SL (A-4)

WT denotes water table.

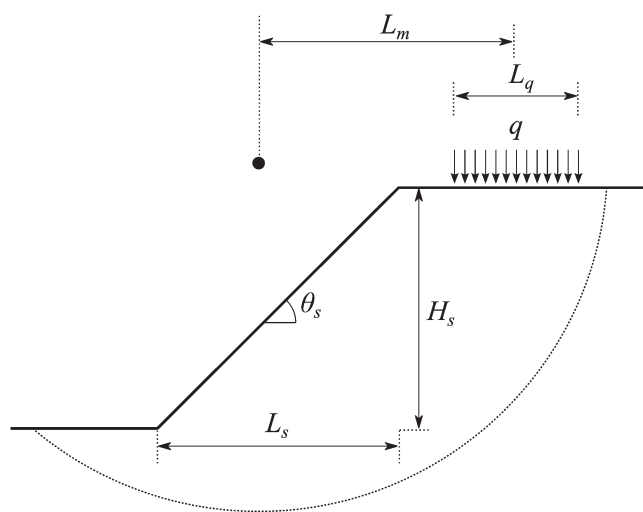


Figure 2.7 Schematic diagram of target slopes.

TABLE 2.3
Geometry of the six slopes

Case	Height H_s (ft)	Length L_s (ft)	Angle θ_s (deg)
A	25.0	70.0	19.7
B	16.5	65.0	14.2
C	21.1	64.3	18.2
D	20.0	65.1	17.1
E	25.6	74.5	19.0
F	17.0	63.5	15.0

TABLE 2.4
Factors of safety from STABL[®] and Geoslope 2007[®] for each case

Case	FS from STABL [®]	FS from Geoslope 2007 [®]
A	2.19	2.33
B	3.02	3.08
C	2.19	2.21
D	1.65	1.64
E	1.53	1.50
F	2.82	2.66

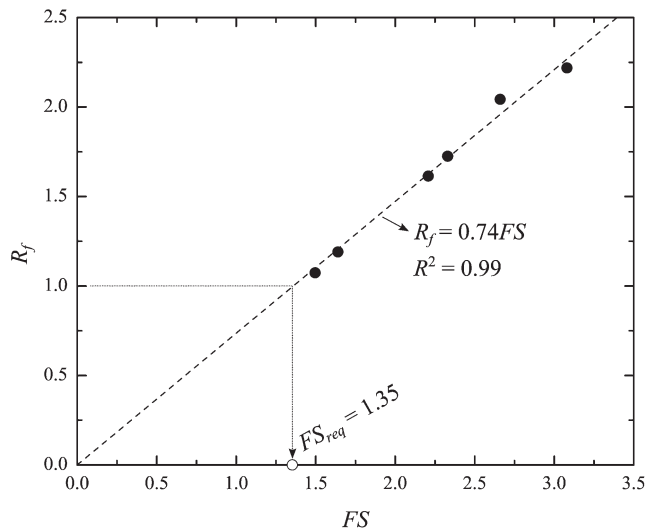


Figure 2.8 Ratio R_f versus FS for $P_{f,T} = 0.01$ (1%).

TABLE 2.5
Analysis results for $P_{f,T} = 0.01$

Case	$M_r(10^5 \text{ lb-ft/ft})$	$M_{rf} (= RF M_r)$ (10^5 lb-ft/ft)	$M_{d,DL}$ (10^5 lb-ft/ft)	$M_{d,LL}$ (10^5 lb-ft/ft)	$M_{df} (= \Sigma LF M_d)$ (10^5 lb-ft/ft)	$R_f (= M_{rf}/M_{df})$	FS
A	464.1	348.1	185.9	13.3	201.8	1.725	2.33
B	133.2	99.9	34.4	8.9	45.0	2.218	3.08
C	95.2	71.4	37.6	5.6	44.2	1.614	2.21
D	52.4	39.3	26.6	5.4	33.0	1.190	1.64
E	29.2	21.9	15.1	4.4	20.4	1.073	1.50
F	104.2	78.1	30.2	6.7	38.2	2.043	2.66

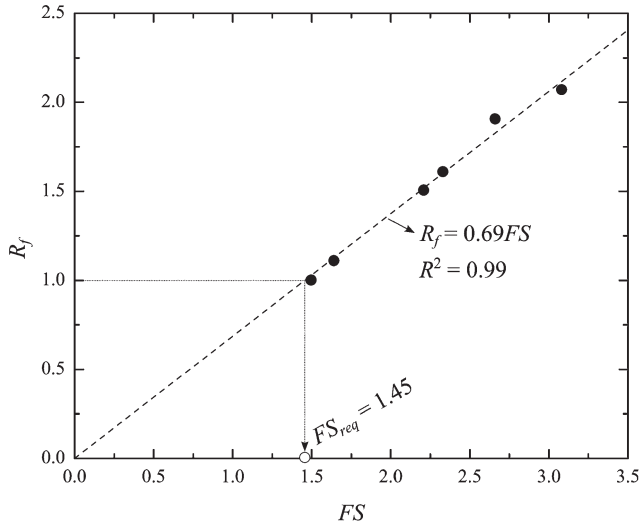


Figure 2.9 Ratio R_f versus FS for $P_{f,T} = 0.001$ (0.1%).

probability is about 1.35 which is within the 1.34-1.40 range of FS^{eq} for undrained slopes subjected to a live load when an appropriate degree of conservatism in the spatial variability of soil properties is considered according to Table 1.3.

Table 2.6 lists the resisting moment M_r , the factored resisting moment M_{rf} , the driving moment $M_{d,DL}$ caused by the dead load, the driving moment $M_{d,LL}$ caused by the live load, the factored driving moment M_{df} , the ratio R_f , and FS for each case when the target probability of failure $P_{f,T}$ is 0.001 (0.1%). For all cases,

the ratio R_f is greater than one, which means that the failure probability P_f is less than the target probability of failure $P_{f,T} (= 0.1\%)$. In case E, which has the lowest FS , the ratio R_f is close to one; the failure probability of the slope in case E is almost identical to the target failure probability, $P_{f,T} = 0.1\%$. Figure 2.9 plots the ratio R_f versus FS ; it shows that the minimum required factor of safety FS_{req} for $P_{f,T} = 0.1\%$ is about 1.45 which is within the 1.40-1.49 range of FS^{eq} for undrained slopes subjected to a live load when an appropriate degree of conservatism in spatial variability of soil properties is considered according to Table 1.3.

Table 2.7 lists the resisting moment M_r , the factored resisting moment M_{rf} , the driving moment $M_{d,DL}$ caused by the dead load, the driving moment $M_{d,LL}$ from the live load, the factored driving moment M_{df} , the ratio R_f , and the factor of safety FS for each case when the target probability of failure $P_{f,T}$ is 0.0001 (0.01%). In case E, the ratio R_f is less than one, meaning that the failure probability of the slope in case E is greater than the target failure probability $P_{f,T} = 0.01\%$. As mentioned before, R_f less than unity means that more than one in ten thousand slopes falling within case E would likely fail. Figure 2.10 plots the ratio R_f versus FS ; it shows the minimum required factor of safety FS_{req} for $P_{f,T} = 0.1\%$ is about 1.56 which is within the 1.44-1.58 range of FS^{eq} for the undrained slopes subjected to a live load when an appropriate degree of conservatism in spatial variability of soil properties is considered according to Table 1.3.

TABLE 2.6
Analysis results for $P_{f,T} = 0.001$

Case	$M_r(10^5 \text{ lb-ft/ft})$	$M_{rf} (= RF M_r)$ (10^5 lb-ft/ft)	$M_{d,DL}(10^5 \text{ lb-ft/ft})$	$M_{d,LL}(10^5 \text{ lb-ft/ft})$	$M_{df} (= \Sigma LF M_d)$ (10^5 lb-ft/ft)	R_f ($= M_{rf}/M_{df}$)	FS
A	464.1	324.9	185.9	13.3	201.8	1.610	2.33
B	133.2	93.2	34.4	8.9	45.0	2.070	3.08
C	95.2	66.6	37.6	5.6	44.2	1.507	2.21
D	52.4	36.7	26.6	5.4	33.0	1.111	1.64
E	29.2	20.4	15.1	4.4	20.4	1.002	1.50
F	104.2	72.9	30.2	6.7	38.2	1.907	2.66

TABLE 2.7
Analysis results for $P_{f,T} = 0.0001$

Case	M_r (10^5 lb-ft/ft)	$M_{rf} (= RF M_r)$ (10^5 lb-ft/ft)	$M_{d,DL}$ (10^5 lb-ft/ft)	$M_{d,LL}$ (10^5 lb-ft/ft)	$M_{df} (= \sum LF M_d)$ (10^5 lb-ft/ft)	$R_f (= M_{rf}/M_{df})$	FS
A	464.1	301.7	185.9	13.3	201.8	1.495	2.33
B	133.2	86.6	34.4	8.9	45.0	1.923	3.08
C	95.2	61.9	37.6	5.6	44.2	1.399	2.21
D	52.4	34.1	26.6	5.4	33.0	1.032	1.64
E	29.2	19.0	15.1	4.4	20.4	0.930	1.50
F	104.2	67.7	30.2	6.7	38.2	1.771	2.66

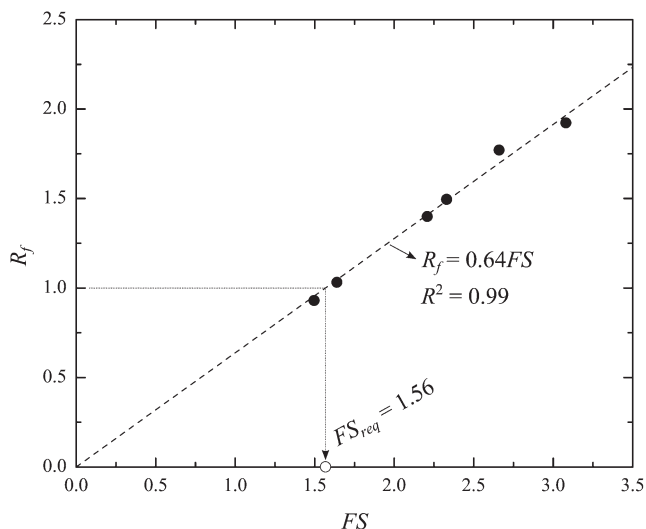


Figure 2.10 Ratio R_f versus FS for $P_{f,T} = 0.0001$ (0.01%).

3. SUMMARY AND CONCLUSIONS

The main goal of this study was to provide more specific guidance on values of resistance factors to implement in load and resistance factor design of slopes, with specific illustrations. Chapter 1 introduced the concepts of load and resistance factors, the target probability of failure for slopes, and the ultimate limit state equation. It then presented a detailed algorithm for resistance factor calculation by using reliability analysis. Chapter 1 then presented calculation examples showing how to implement LRFD in slope stability analysis. Six slopes were constructed by using both drained and undrained shear strengths. The nominal values of controlling parameters (c (s_u), ϕ and γ), the resistance and load factors, and the equivalent factor of safety at three target probabilities of failure were presented. In addition, the effect of slope geometry was discussed in Chapter 1. It was shown that, when realistic values of COV and scale of fluctuation of the soil properties were assumed (values close to those of set D), the resulting RF^* values did not depend strongly on slope geometry, suggesting that rigorous reliability analysis algorithm proposed in the present study can be used effectively to produce load and resistance factors for use in design of slopes.

Chapter 2 applied the LRFD methodology summarized in Chapter 1 to check the stability of a total of six slope cases (case A through F) provided by INDOT. The short-term (undrained) properties of soil were used to analyze all cases. For all the adopted target probabilities of failure, there was a strong linear correlations between the ratio R_f of factored resistance to factor load and FS . In all cases, the minimum required factor of safety FS_{req} was within the range of FS^{eq} for the undrained slopes subjected to a live load established by Salgado and Kim (19).

From the successful implementation in this study, the recommended resistance factors RF^* adjusted with respect to the proposed load factors LF^* ($LF^*_{DL} = 1.0$ and $LF^*_{LL} = 1.2$) are 0.75, 0.70, and 0.65 for $P_{f,T}$ of 0.01 (1%), 0.001 (0.1%), and 0.0001 (0.01%), respectively. Of these, the value of 0.70 would appear to better match the current level of reliability with which INDOT is comfortable.

REFERENCES

- Basu, D., and R. Salgado. Load and Resistance Factor Design of Drilled Shafts in Sand. *Journal of Geotechnical and Geoenvironmental Engineering*, ASCE, Vol. 138, No. 12, 2012, pp. 1455–1469.
- AASHTO. *Standard Specifications for Highway Bridges* (17th ed). American Association of State Highway and Transportation Officials, Washington, D.C., 2002.
- Yu, H. S., R. Salgado, S. Sloan, and J. Kim. Limit Analysis vs. Limit Equilibrium for Slope Stability Assessment.” *Journal of Geotechnical and Geoenvironmental Engineering*, Vol. 124, No. 1, 1998, pp. 1–11.
- Kim, J., R. Salgado, and H. S. Yu. Limit Analysis of Soil Slopes Subjected to Porewater Pressures.” *Journal of Geotechnical and Geoenvironmental Engineering*, Vol. 125, No. 1, 1999, pp. 49–58.
- Kim, J., R. Salgado, and J. Lee. Limit Analysis of Complex Soil Slopes. *Journal of Geotechnical and Geoenvironmental Engineering*, Vol. 128, No. 7, 2002, pp. 546–557.
- Loukidis, D., P. Bandini, and R. Salgado. Comparative Study of Limit Equilibrium, Limit Analysis and Finite Element Analysis of the Seismic Stability of Slopes. *Geotechnique*, Vol. 53, No. 5, 2003, pp. 463–479.
- Chowdhury, R., and P. N. Flentje. Role of Slope Reliability Analysis in Landslide Risk Management. *Bulletin of Engineering Geology and the Environment*, Vol. 62, 2003, pp. 41–46.

8. Christian, J. T., C. C. Ladd, and G. B. Baecher. Reliability Applied to Slope Stability Analysis. *Journal of Geotechnical and Geoenvironmental Engineering*, Vol. 120, No. 12, 1994, pp. 2180–2207.
9. Loehr, J. E., C. A. Finley, and D. Huaco. *Procedures for Design of Earth Slopes Using LRFD*. Report No. OR 06-010. University of Missouri–Columbia and Missouri Department of Transportation, 2005, p. 80.
10. Santamarina, J., A. Altschaeffl, and J. Chameau. Reliability of Slopes: Incorporating Qualitative Information. In *Transportation Research Record: Journal of the Transportation Research Board*, No. 1343, Transportation Research Board of the National Academies, Washington, D.C., 1992, pp. 1–5.
11. Bishop, A. W. The Use of the Slip Circle in the Stability Analysis of Slopes. *Geotechnique*, Vol. 5, 1955, pp. 7–17.
12. Spencer, E. A Method of Analysis of the Stability of Embankments Assuming Parallel Inter-slice Forces. *Geotechnique*, Vol. 17, No. 1, 1967, pp. 11–26.
13. Salgado, R. *The Engineering of Foundations*. McGraw-Hill, New York, 2008.
14. Robinson, D. G. *A Survey of Probabilistic Methods Used in Reliability, Risk and Uncertainty Analysis: Analytical Techniques I*. Sandia Report, SAND98-1189. Sandia National Laboratories, Albuquerque, New Mexico, 1998.
15. Rosenblatt, M. Remarks on a Multivariate Transformation. *Annals Mathematical Statistics*, Vol. 23, No. 3, 1952, pp. 470–472.
16. Hohenbichler, M., and R. Rackwitz. Non-normal Dependent Vectors in Structural Safety. *Journal of the Engineering Mechanics Division*, Vol. 107, No. 6, 1981, pp. 1227–1238.
17. AASHTO. *LRFD Bridge Design Specifications* (4th ed.). American Association of State Highway and Transportation Officials, Washington, D.C., 2007.
18. Lansivara, T., and T. Poutanen. Slope Stability with Partial Safety Factor Method. Presented at the 19th International Conference on Soil Mechanics and Geotechnical Engineering, Paris, France, 2013.
19. Salgado, R., and D. Kim. Reliability Analysis and Load and Resistance Factor Design of Slopes. *Journal of Geotechnical and Geoenvironmental Engineering*, Vol. 140, No. 1, 2013, pp. 57–73. doi: [10.1061/\(ASCE\)GT.1943-5606.0000978](https://doi.org/10.1061/(ASCE)GT.1943-5606.0000978).

About the Joint Transportation Research Program (JTRP)

On March 11, 1937, the Indiana Legislature passed an act which authorized the Indiana State Highway Commission to cooperate with and assist Purdue University in developing the best methods of improving and maintaining the highways of the state and the respective counties thereof. That collaborative effort was called the Joint Highway Research Project (JHRP). In 1997 the collaborative venture was renamed as the Joint Transportation Research Program (JTRP) to reflect the state and national efforts to integrate the management and operation of various transportation modes.

The first studies of JHRP were concerned with Test Road No. 1—evaluation of the weathering characteristics of stabilized materials. After World War II, the JHRP program grew substantially and was regularly producing technical reports. Over 1,500 technical reports are now available, published as part of the JHRP and subsequently JTRP collaborative venture between Purdue University and what is now the Indiana Department of Transportation.

Free online access to all reports is provided through a unique collaboration between JTRP and Purdue Libraries. These are available at: <http://docs.lib.purdue.edu/jtrp>

Further information about JTRP and its current research program is available at: <http://www.purdue.edu/jtrp>

About This Report

An open access version of this publication is available online. This can be most easily located using the Digital Object Identifier (doi) listed below. Pre-2011 publications that include color illustrations are available online in color but are printed only in grayscale.

The recommended citation for this publication is:

Salgado, R., S. I. Woo, F. S. Tehrani, Y. Zhang, and M. Prezzi. *Implementation of Limit States and Load Resistance Design of Slopes*. Publication FHWA/IN/JTRP-2013/23. Joint Transportation Research Program, Indiana Department of Transportation and Purdue University, West Lafayette, Indiana, 2013. doi: 10.5703/1288284315225.